

LL16
X-39
NACA TN 2843

2843



NATIONAL ADVISORY COMMITTEE FOR AERONAUTICS

TECHNICAL NOTE 2843

AUXILIARY EQUIPMENT AND TECHNIQUES FOR ADAPTING THE
CONSTANT-TEMPERATURE HOT-WIRE ANEMOMETER TO
SPECIFIC PROBLEMS IN AIR-FLOW MEASUREMENTS

By James C. Laurence and L. Gene Landes

Lewis Flight Propulsion Laboratory
Cleveland, Ohio



Washington
November 1952

AFMDC
TECHNICAL NOTE
2843

310, 98/39



0065677

IQ

NACA TN 2843

TABLE OF CONTENTS

	Page
SUMMARY	1
INTRODUCTION	
CONSTANT-TEMPERATURE HOT-WIRE ANEMOMETER AND AUXILIARY EQUIPMENT	3
Constant-Temperature Anemometer	3
Auxiliary Equipment	5
Average-square computer	5
Supplementary heating current	6
Double-correlation computer	7
STANDARDIZATION AND CALIBRATION OF HOT-WIRE PROBES	7
Calibration Facilities	8
Wires and Mounting Techniques	8
Heat Loss from Wires	10
FLUCTUATION MEASUREMENTS	12
Fundamental Definitions	12
Periodic Phenomena	13
Frequency measurements	14
Velocity profiles	14
Compressor surge and rotating stall	14
Nonperiodic Phenomena	15
Intensity of turbulence	15
Spectrum of turbulence	16
Scale of turbulence	16
APPENDIXES	
A - SYMBOLS	18
B - THEORY OF AVERAGE-SQUARE COMPUTER	21
C - OPERATION INSTRUCTIONS	22
D - CALIBRATION OF ELECTRONIC EQUIPMENT	25
E - REDUCTION OF DATA	26
F - DERIVATION OF EQUATION FOR INTENSITY	31
G - MEASUREMENT OF CORRELATION COEFFICIENT AND SCALE OF TURBULENCE BY TWO-WIRE METHOD	33
REFERENCES	34

TABLES

I - HOT-WIRE MATERIALS RATED ACCORDING TO SOME DESIRABLE PHYSICAL PROPERTIES AND AVAILABILITY	36
II - COMPARISON OF WIRE DIAMETERS OBTAINED BY THREE DIFFERENT METHODS	36
III - COMPARABILITY OF HOT-WIRE ANEMOMETER PROBES	37

TECHNICAL NOTE 2843

AUXILIARY EQUIPMENT AND TECHNIQUES FOR ADAPTING THE CONSTANT-
TEMPERATURE HOT-WIRE ANEMOMETER TO SPECIFIC PROBLEMS IN
AIR-FLOW MEASUREMENTS

By James C. Laurence and L. Gene Landes

SUMMARY

The constant-temperature hot-wire anemometer amplifier and accessories have been developed to provide an instrument with wide frequency response, good stability, and ease of operation. Auxiliary equipment has been developed to provide heating currents for large wires, to make average-square computations, and to make double-correlation coefficient measurements.

Techniques are described for using this equipment to study periodic phenomena such as surge, rotating stall, and wake surveys in centrifugal- and axial-flow compressors. The application of the equipment to the study of nonperiodic phenomena such as intensity, scale, and spectra of isotropic turbulence is also discussed.

Heat-loss data for standardized tungsten wire probes show that no wire calibration is necessary if accuracies of ± 5 percent are sufficient.

INTRODUCTION

The problems associated with the evaluation of compressor and turbine performance, as well as the flow fluctuations in combustion phenomena, are of such a nature that a knowledge of the instantaneous flow patterns is of considerable importance. These measurements in many cases are beyond the range of conventional measuring instruments because of the limitations of frequency response. Measurements of this type (compressor surge and rotating stall, blade wake velocity profiles, vortex shedding frequencies, and associated phenomena) are most readily made by means of hot-wire anemometers.

The advantages and disadvantages of operating hot-wire anemometers at constant current and at constant resistance (temperature) have been discussed by several writers (references 1 to 3).

The principal advantages of the constant-temperature system are as follows: (1) It provides a continuously varying feedback voltage which operates the wire with continuous compensation, (2) it can be used for large mass-flow fluctuations - over 100 percent of the mean flow, (3) in instances where there is a sudden decrease in flow there is no danger of wire burnout. The problems of air-flow fluctuations associated with compressors, turbines, combustion phenomena, and so forth usually involve flow changes which are large with respect to mean flow. Experience shows that the fluctuations found in jet-engine research are usually larger than 1 to 2 percent and hence the main disadvantage of the constant-temperature hot-wire anemometer, its relatively large input noise level, is unimportant in measurements of this kind.

An amplifier design incorporating these advantages was proposed in reference 2. This anemometer utilizes a constant-temperature feedback system employing a very stable direct-coupled amplifier of wide frequency response. Instruments built according to this design are in operation at the NACA Lewis laboratory and have been applied to the measurement of fluctuating flows of several kinds.

As in constant-current hot-wire anemometry, it is most often convenient to study the signal from the hot wire (after compensation and amplification) on the cathode-ray oscilloscope screen. If the fluctuation pattern shows no periodic components, the analysis of the flow is usually conducted on the basis of the statistical theory of turbulence. If the oscillogram has some periodic components, the absolute magnitude of the flow changes is most often of interest.

In the statistical theory of Taylor (reference 4), the intensity, the spectrum, and the scale of turbulence are of importance. In order to study the intensity of turbulence, usually defined as the root-mean-square value of the velocity fluctuations, an average-square computer was developed. This instrument utilizes an electronic circuit to give a meter reading which is directly proportional to the average square of the input voltage regardless of wave form within its frequency limits.

If the velocity fluctuations at two points within the flow are to be compared, the statistical theory makes use of the correlation coefficient to define the scale of turbulence. These measurements are facilitated by use of an electronic circuit which gives the ratio of the average squares of the sums and differences of the signals from two hot wires.

If the frequency-response requirements are not too great, wires of greater diameter can be used in installations where dirt, oil, or other foreign particles cause excessive wire breakage. Large-diameter wires require larger heating currents for operation than the commonly used 0.0002-inch wires. Since the constant-temperature amplifiers used supply, at most, approximately 150 milliamperes of current, an auxiliary direct-current supply is used which supplements the electronically controlled supply.

In normal use of hot-wire equipment in rotating machinery, experience has shown that wires are subject to frequent damage. The individual calibration for heat loss becomes expensive and time consuming. Thus, one of the principal aims of this work was to standardize, insofar as possible, the equipment described in order that measurements could be made with a minimum amount of wire calibration. It was necessary to investigate the heat-loss data from wires in the range of Mach number and Reynolds number which are not found in the literature. Reference 5 shows the ranges which have been covered for wires in cross flow. Accordingly, the results in the Mach number range 0 to 0.3 and Reynolds number range 4 to 64 based on wire diameter, free-stream density, and film temperature are published herein. Some additional data on the effect of temperature difference between the wire and the stream on the heat lost by the wire are also included.

CONSTANT-TEMPERATURE HOT-WIRE ANEMOMETER AND AUXILIARY EQUIPMENT

Constant-Temperature Anemometer

Many of the transient phenomena studied by the hot-wire anemometer are of high frequency - several thousand cycles per second. For example, blade wake passages in compressors and turbines represent frequencies as high as 10,000 cycles per second with associated frequencies several times greater. Consequently, a desirable characteristic of a hot-wire anemometer is a frequency response in the range of 30,000 to 40,000 cycles per second. Conventional constant-current hot-wire anemometers seldom exceed 10,000 to 20,000 cycles per second.

The components of the hot-wire anemometer which determine the frequency response are the amplifier, the bridge, the connecting cables, and the probes. The contribution of each of these factors in the system to be described will be explained in the following paragraphs.

The amplifier uses a very stable, direct-coupled circuit described in reference 2. A photograph of the amplifier is shown in figure 1; its schematic diagram is given in figure 2 and its frequency response, in figure 3. This figure shows an essentially flat response from direct current to 80,000 cycles per second.

The difficulty of compensating for the lag in response of a hot wire is due to the fact that the time constant is a function of the flow conditions as well as of the physical properties of the wire. For this reason the amplifier described is operated with negative feedback through a bridge circuit to provide instantaneous compensation for the varying wire time constant. Figure 4 shows the theoretical relation between the wire response and the voltage to be fed back to insure correct compensation.

To insure correct operation of the amplifier, it was necessary to design a Wheatstone bridge (in which the wire is one of the arms) which would not cause instability in the amplifier and would have a flat frequency response to at least 50 kilocycles and preferably much higher. The bridge was constructed as shown in figure 5. This is a fixed-ratio bridge which is used in the negative feedback loop of the amplifier to keep the operating resistance of the hot wire constant.

2640

The resistors used in the arms of the bridge are a special type with an impedance that does not vary over the frequency range from direct current to 200 kilocycles per second. Bridges have been made with resistors which have a smaller frequency range over which their impedance is constant with frequency, but for such bridges the connecting cables must be shorter.

The geometry of the bridge, in addition to the inductance of the resistors, was found to affect its response. In general, a symmetrical arrangement was found best. The wires used to make connections within the bridge were carefully matched as to length and resistance. Each of the ground connections was brought out directly to a single terminal which could be grounded wherever desired.

The cables are made of coaxial cable with a capacitance of 13 micro-microfarads per foot. In the present design, because of cable capacitance, the length is limited to 15 feet.

The unbalanced voltage from the bridge can be observed at distances up to 100 feet from the bridge by means of the same type of coaxial cable without apparent difficulty. The reading of the bridge current at the same distance, 100 feet from the amplifier, was obtained by wiring a precision 1-ohm resistor in series with the bridge current meter and observing the potential drop across this resistor by means of a voltmeter and coaxial cable.

The shielding of bridge, cables, and probes is important to minimize 60-cycle pickup. Adequate grounding at several points in the instrument layout and shielding of connectors are of help in eliminating this extraneous signal.

2640 In order to prevent instability in the amplifier, which usually leads to wire burnout, some alterations in the conventional probe design were necessary. Since the distributed capacitance of the leads from bridge to amplifier and from bridge to probe is quite critical, it was found necessary to substitute coaxial cable for the customary leads as well as for the internal leads of the probe itself. The probe, shown in figure 6(a), is a low-temperature probe with the maximum temperature to which it can be exposed determined by the melting point of the polystyrene insulation (about 180° F) in the coaxial cable. The result of the use of the coaxial cable in the probe was a decrease in the capacitance of the conventional probe by a factor of 10. It is possible to use wires with diameters as small as 0.000125 inch mounted on these probes.

The design of a probe for use under conditions of ambient temperature much higher than 180° F is shown in figure 6(b). In this probe the coaxial cable is replaced by a ceramic insulator with a single wire through its center. The Inconel tube itself is used for the second conductor, which is grounded. The capacitance is, of course, greater than that of the probe of figure 6(a), but it is still low enough for operation with wires of size down to 0.000125 inch. Since all probe connections are silver-soldered, this probe can be used at high temperatures.

In many types of rotating machinery, the direction of the fluctuating air stream is generally axial and parallel to cylindrical surfaces. In these circumstances a wire mounted parallel to the axis of the probe is desirable. A sketch of such a probe is shown in figure 6(c).

Measurements of the frequency response of the complete system (amplifier, bridge, cables, and probe) were made as indicated in figure 7. The small bridge unbalance plotted in figure 8 is fairly constant to 40,000 cycles per second, which is the limit of flat response of the anemometer. This figure indicates that the voltage fed back compensates for the lag in wire response up to 20,000 cycles per second. Further changes in the curve beyond this point are probably due to phase shift in the amplifier.

Auxiliary Equipment

Average-square computer. - In turbulence measurements the hot-wire signals usually are nonsinusoidal and may be nonrepetitive. An ordinary voltmeter therefore will not correctly measure the average-square value of these signals. Although a thermocouple-type voltmeter could be used, it cannot withstand overloads such as transient turbulence might introduce and it does not have sufficient range. Hence an electronic average-square computer was developed. The principal requirement of this computer is to make average-square measurements of aperiodic signals varying from 10 millivolts to 3 volts.

By the use of two tubes with their plate circuits connected in push-pull, as shown in the block diagram of figure 9, the static direct-current component may be balanced out. It has been shown (reference 6) that for some vacuum tubes having effectively coplanar control grids, there is a change of direct-current component of plate current proportional to the product of the control grid voltages and the cosine of their phase angle. The vacuum tubes will saturate during operation so that a direct-current voltmeter which is used to measure the output will be protected during overloads. Since a direct-current meter is used in the output, alternating-current components of the plate current can be ignored. If the two control grid voltages are in phase for both tubes, the direct-current component of plate current, proportional to the square, will be canceled. Therefore, these grid voltages are fed 180° out of phase for one of the tubes. The squared output is then merely twice the value for one tube. (See appendix B. The symbols used in appendix B and elsewhere throughout the report are defined in appendix A.) A detailed schematic diagram of the computer is shown in figure 10.

The frequency response of the computer is flat to approximately 2 percent from 10 to 20,000 cycles per second (see fig. 11). Its accuracy is better than 2 percent of full scale for all ranges except the two lowest decades (amplifier near maximum gain); the error for the two lowest decades is less than 4 percent (see fig. 12). Once the computer has been stabilized it will remain zeroed to within 1 percent of full scale for several hours.

Supplementary heating current. - The constant-temperature anemometer described in this report has a maximum usable current output of 150 milliamperes. An auxiliary direct-current supply may be used to supplement this current if the mass-flow fluctuations are not so large compared with the mean value that decreases in mass flow would leave the wire overheated by the supplementary current. A battery power supply is used for this application because of its low noise level and simplicity of operation. To prevent loading effects on the bridge, it is necessary that the source impedance of the external supply be large compared with that of the bridge. The series resistors (fig. 13) perform this function as well as providing a means of current control.

The output of the auxiliary current supply is connected in parallel with the output of the constant-temperature hot-wire anemometer. (For operating instructions, see appendix C, Auxiliary Current Supply.)

This method of operation has been successfully used with platinum-iridium wires 0.001 inch in diameter and 0.1 inch in length. The wire was operated with currents from 150 to 250 milliamperes (approximately 1100° F). For this operation, over one-half the current was supplied by the external supply.

2640

Double-correlation computer. - In order to study the velocity fluctuations at two points within an air stream, a double-correlation computer was designed which gives a meter reading indicating the ratio of the average squares of the sums and differences of the outputs from two hot-wire anemometers. Since the average-square computer performs a part of this operation it was required to take the sum and the difference and the ratio of the sums and differences. The adding circuit is a twin-triode type of mixing circuit (fig. 14) with calibrating potentiometers at the inputs. The difference circuit utilizes the same principle except that one of the inputs must have its phase reversed. This function is performed by a triode amplifier operating with nearly 100 percent negative feedback. When all four circuits are adjusted to have the same gain, the calibration is complete if identical signals fed into the sum circuit give an output twice the input (actually the sum of the inputs) and those fed into the difference circuit give a minimum output (a null setting for either gain control). Details of the complete circuit are given in figure 15.

A direct-current type of ratio meter is used to measure the ratio of the outputs from two average-square computers. The double-correlation apparatus is used in conjunction with two hot-wire anemometers for obtaining the scale of turbulence. The reading of the ratio meter may be used in equation (G7) (see appendix G) to obtain the correlation coefficient and the scale of turbulence can be calculated on the basis of the statistical theory of turbulence.

The accuracy of the unit is primarily a function of the gain of the amplifiers. This gain is constant to approximately 10 percent from 10 to 20,000 cycles per second (fig. 16). Since the vacuum tubes are operated at low levels and therefore on the linear portion of their characteristic curves, the variation of gain with different amplitudes of input signal is negligible. An experimental plot of this deviation is shown in figure 17.

STANDARDIZATION AND CALIBRATION OF HOT-WIRE PROBES

The sensitive element in the hot-wire anemometer is a fine wire (tungsten, platinum-iridium, nickel) which must be properly mounted on a probe for support and then calibrated for heat loss in an air stream. In order to standardize the mounting and calibration of these wires, a program was planned to investigate:

- (1) The effect of Mach number and Reynolds number on the convective heat loss for the ranges not previously published (references 5, 7, and 8)

- (2) The repeatability of calibration of tungsten wire probes with continued use
- (3) The uniformity of calibration of tungsten wire probes
- (4) The end-loss corrections to compensate for conduction to the prongs
- (5) The effect of temperature difference between the wire and the air stream on the calibration of the wires

2640

Calibration Facilities

A specially designed low-turbulence duct was built for use in this investigation and for future hot-wire calibration work. The test section has a square cross section 3.6 by 3.6 inches and extends for a total length of 40 inches. This test section is provided with expandable walls, removable inlet screens of various mesh sizes, static-pressure taps along the walls, and a number of test stations on all sides for the insertion of probes. Windows are provided for the use of schlieren apparatus and an interferometer.

The plenum chamber has a smooth exit cone through which the air is accelerated to the test-section entrance. Located in this chamber are a filter, consisting of a thick layer of felt which removes dirt particles which might break the wires, and also five screens to smooth out the air flow.

Another filter is included in the air lines ahead of the plenum chamber. The function of this filter is the removal of large pieces of pipe scale, oil particles, and so forth.

The Mach number and mass-flow ranges at the test section were 0 to 0.8 and 0 to 130 pounds per square foot per second, respectively, and the temperature of the supply air could be varied from -20° to 130° F.

Wires and Mounting Techniques

The selection of a hot-wire material for a given installation is governed by temperature coefficient of resistance, tensile strength, temperature at which oxidation occurs, time constant of the wire, and availability of the material. Table I is a comparison of the commonly used materials rated according to these properties. Most of these materials can be drawn to approximately 0.0004-inch diameter. For smaller diameter wires, however, etched tungsten, and Wollaston processed platinum, platinum-iridium, and nickel are available. Except for its low resistance to oxidation (serious above 600° F), the favorable rating

of tungsten in table I shows it to be a desirable material for hot-wire anemometry and therefore the most frequently used material for low ambient temperatures. For use where ambient temperatures are high, platinum-iridium is most suitable.

The proper mounting of tungsten wires is accomplished by copper-plating the ends of the wire at the points where the soldering is to take place. This technique, originated by the National Bureau of Standards (reference 9) and improved upon later (reference 10), makes it possible to soft-solder or silver-solder the wires to the prongs. All other wire materials can be easily soft-soldered or silver-soldered. An initial tension can be applied to the wire by a spring device as described in reference 7, or by a weight hung on the wire before it is fastened to the prongs.

Of the methods used to measure the diameter of the very small wires, only two have proved satisfactory: (1) photomicrography of the wire with the electron microscope, and (2) calculation of an average diameter based on the resistance of a given length of the wire.

Since $R = \sigma l/S$, it is possible to calculate an average diameter, assuming a circular cross section and using a value of the resistivity found in the literature. The diameters of some larger wires have been measured by means of a measuring microscope. The results of these measurements are found in table II.

The problem of obtaining standardized probes with a more uniform cold resistance and a predictable calibration curve was the subject of much experimentation. It has been found that of all the variables encountered in probe fabrication the most difficult one to control is the wire diameter. The sizes of tungsten which have been used - 0.0002, 0.00014, and 0.000125 inch - are produced by etching drawn wire of 0.0004-inch diameter until the desired size is obtained. The supplier of the wire used for these tests has been unable to control the diameter of the wire produced by this method to better than ± 8 to ± 10 percent except by careful selection. The most careful selection and control still result in a variation of diameter (checked by the second of the two described methods) of ± 5 percent. Electron micrographs of etched tungsten wires are shown in figure 18. In this photograph, samples A and C are wires which are being used at present, whereas sample B was recently obtained from another manufacturer. The diameters as reported by the manufacturer of samples A and C were calculated from the resistance of a given length of the wire and are in considerable variation from actual measurements taken from these electron micrographs. Since the diameter enters the Reynolds number calculations, the ordinary probes may be expected to show a variation of about 10 percent in calibration.

Other methods of producing fine wires have been considered and will be the subject of further research. Two of these are the electro-polishing technique (reference 11) and the evaporation method in which metal is evaporated from the surface of the wire in a vacuum. Either or both of these methods promise a more rigid control of wire diameter than the etching process and further work will be done to establish the feasibility of manufacturing wires by these methods.

Heat Loss from Wires

2640

The constant resistance method of operation was used for all wire calibration tests. In order to maintain the wire at a constant mean resistance, an automatic balancing Kelvin bridge was constructed which reduced the data-taking time considerably. In all calibration runs the resistance of the wire was so adjusted that the average temperature of the wire was in the range 500° to 600° F except for those runs in which the effect of temperature difference was being investigated.

The methods of evaluating hot-wire data (calculation of Nusselt, Prandtl, and Reynolds numbers used in the graphs presented) were the same as those used in reference 7. For example, thermal conductivity, viscosity, and specific heat at constant pressure were evaluated at the film temperature, which is assumed to be the arithmetic average of the wire recovery temperature and the wire operating temperature. The density, however, was calculated at the free-stream static temperature and static pressure. Reference 7 contains a very complete discussion of the methods used in evaluating the data as well as the method for correcting the data for end losses to the prongs by conduction.

The data for a long wire ($l/d = 2500$, effectively infinite) is presented in a series of curves grouped to show the effect of Mach number, the effect of temperature difference on the calibration, and a comparison with data reported by other investigators. Corrections for end losses were negligible for these data. Figure 19 gives conventional calibration curves for hot-wire anemometer use. These curves show quite clearly the influence of Mach number and temperature difference on the heat lost by the wire to the air stream and agree very well with the data reported in reference 7 as well as with the data reported by McAdams (reference 8) within the limits of uncertainty of the wire diameter.

An equation for the relation among Reynolds, Nusselt, and Prandtl numbers at a Mach number of 0.3 and a wire temperature of 343° F (fig. 19(b)) is

$$\frac{Nu_f}{Pr_f^{0.3}} = 0.21 + 0.57 Re^{0.5} \quad (1)$$

When this equation is considered as an average equation for the range of Mach number and wire temperature, the maximum deviation of a data point in figure 19 is about ± 7 percent. For the same range of Reynolds number, McAdams (reference 8, p. 222) recommends

$$\frac{Nu_f}{Pr_f^{0.3}} = 0.35 + 0.47 Re^{0.52} \quad (2)$$

2640

Figure 20 shows the comparison of all the data points in figure 19 with equation (2). The probes used for this part of the investigation were not conventional, since the l/d was very large.

Heat-loss data for conventional size hot-wire probes ($l/d = 400$) are shown in figures 21 and 22. Figures 21 and 22 also show the effect on the heat-loss rate of the temperature difference between the wire and the air stream. Because of the lower value of l/d , these data are corrected for end losses by the method described in reference 7. The data are presented in two different plots because of the usefulness of the information. Thus, in figure 21 it is possible to select a calibration curve corresponding to a temperature difference encountered in a testing situation. For example, if the recovery temperature is 200° F, an operating wire temperature of 300° F or greater is needed to provide adequate sensitivity, and the appropriate calibration curve can be chosen from this figure. In like manner, figure 22 shows typical operating curves for standardized probes and is useful in determining an operating current necessary to obtain a desired temperature difference.

The results of a controlled experiment on one group of six probes are shown in table III and figure 23. This and similar experiments have established that the calibration of the standard tungsten hot-wire probe can be predicted to within ± 5 percent. In many instances this degree of accuracy is sufficient if the other variables involve errors at least that large. If this degree of accuracy is sufficient, the calibration procedure is thus reduced to a single resistance measurement at a known temperature. This can be a measurement with no flow. One word of caution, however, should be given. There may be variables in any given testing situation which, if uncontrolled or unspecified, might cause large errors when the standard calibration curve is used. Thus, if the direction at which the air stream crosses the wire is different from that in the calibration setup (usually normal to the wire), the use of the calibration curve will result in errors. In many types of rotating machinery the direction of the air stream, particularly during flow fluctuations, is difficult to predict. In this case a probe should be used (fig. 6(c)) which will ensure that the major fluctuations of the air stream pass normal to the wire.

Evidence is presented in figure 24 which shows that the end-loss correction for a standard probe is not sufficient to bring the heat-loss curve into agreement with that of a wire in which the end losses are negligible. At present the explanation of this discrepancy may be that the lack of knowledge of wire diameter is causing the disagreement. In experiments using larger wires where the diameter is well known, the correction is sufficient to bring the two curves into agreement. The experiment which resulted in this data was as follows: Heat-loss data for a standard hot-wire probe with a length-to-diameter ratio of 400 were obtained in the usual manner. The data were corrected for end losses to the prongs by two methods (references 7 and 12). Heat-loss data were obtained for a specially built probe where the length-diameter ratio was 2500. Figure 24 shows a comparison of the data obtained for these probes.

2640

FLUCTUATION MEASUREMENTS

Fundamental Definitions

Two parameters of prime importance in the statistical theory of turbulence are the intensity and the scale of turbulence (reference 13). The intensity of turbulence is defined as the ratio of the root mean square of the velocity fluctuations to the mean velocity. Thus, if u , v , and w are the components of the velocity fluctuations,

$$\text{Intensity in direction of flow} = \frac{\sqrt{u^2}}{U}$$

$$\text{Intensity normal to direction of flow} = \frac{\sqrt{v^2}}{U}$$

$$\text{Intensity normal to direction of flow and normal to } v = \frac{\sqrt{w^2}}{U}$$

$$\text{In isotropic turbulence, } \overline{u^2} = \overline{v^2} = \overline{w^2}.$$

The scale of turbulence is defined from the correlation between the velocity fluctuations at two points in the air stream. From the statistical definition of the correlation coefficient,

$$\left. \begin{aligned} \alpha_x &= \frac{\overline{u_{x,1} u_{x,2}}}{\sqrt{\overline{u_{x,1}^2} \sqrt{\overline{u_{x,2}^2}}}} \quad (\text{longitudinal correlation coefficient}) \\ \alpha_y &= \frac{\overline{u_{y,1} u_{y,2}}}{\sqrt{\overline{u_{y,1}^2} \sqrt{\overline{u_{y,2}^2}}}} \quad (\text{lateral correlation coefficient}) \end{aligned} \right\} (3)$$

From these two values, the longitudinal scale and lateral scale are defined as

$$\left. \begin{aligned} L_x &= \int_0^\infty \mathcal{R}_x dx \quad (\text{longitudinal scale}) \\ L_y &= \int_0^\infty \mathcal{R}_y dy \quad (\text{lateral scale}) \end{aligned} \right\} \quad (4)$$

In hot-wire measurements, the value of the scale as defined here can be obtained by measurements of the correlation coefficient. This method requires the simultaneous measurement of the velocity fluctuations at two locations by means of a multiple-wire setup.

As shown in reference 14, it is possible to relate the longitudinal scale to the energy spectrum of turbulence. This relation takes one of two forms, depending upon the method used in making the spectrum measurements. If an appropriate low-pass filter is used in conjunction with the average-square computer, this relation is

$$\frac{\overline{u_{n,h}^2}}{\overline{u_t^2}} = \frac{2}{\pi} \tan^{-1} \frac{2\pi L_x n_h}{U} \quad (5)$$

where $\overline{u_{n,h}^2}$ is the energy in the spectrum from zero frequency to n_h , the cut-off frequency; and $\overline{u_t^2}$ is the total energy in the spectrum when all frequencies are being passed by the filter. But if a band-pass filter is used, the relation becomes

$$\frac{\overline{u_n^2}}{\overline{u_t^2}} = \frac{\frac{4L_x}{U}}{1 + \left(\frac{2\pi L_x}{U}\right)^2 n^2} \quad (6)$$

where now $\overline{u_n^2}$ is the energy per unit frequency interval at a discrete frequency n and $\overline{u_t^2}$ is again the total energy in the turbulence spectrum (the area under the curve).

Periodic Phenomena

Figure 25 shows typical block diagrams of hookups of the hot-wire anemometer and suitable electronic equipment for recording or observing the periodic phenomena.

Frequency measurements. - Periodic fluctuations in air flow, such as vortices shed by cylinders and flame holders (reference 15), blade wakes in rotating machinery (compressors and turbines), and so forth, can be studied by means of the hot-wire anemometer. For these measurements the apparatus connections are shown in figure 25(a). The periodic phenomenon under study is picked up by the hot wire and the amplifier output is placed on the cathode-ray oscilloscope y-axis amplifier. A standard audio oscillator is connected to the oscilloscope x-axis amplifier and the frequency of the periodic signal is given by the resulting Lissajous figure formed on the screen.

The signal from the hot-wire anemometer can be led to a frequency meter, which gives the frequency directly. This has not, in general, tended to be as satisfactory a procedure as the method using the Lissajous figures.

Velocity profiles. - A survey of wakes from various shapes of centrifugal compressor blade can be obtained by use of a hot-wire anemometer. The wire may be placed at chosen positions at the exit of the impeller to obtain the velocity profiles (actually, mass flow).

A block diagram of a typical setup is shown in figure 25(b). The decade amplifier serves the dual purpose of preamplifier and isolation amplifier at the anemometer location. This serves to isolate the anemometer from the long line to the control room where the oscilloscope and recording camera are located. A variable-frequency electronic filter is used to eliminate unwanted components of this signal. Since the frequency with which the blades pass the wire is about 1000 cycles per second, frequencies below a few hundred cycles are not of much interest. The external synchronizing signal is produced by a small permanent magnet and coil mounted near the rotor shaft. This permits the viewer to see only a few blade passages for each revolution instead of all the passages.

Evaluation of the data will require the following information: overall instrumentation gain (see appendix D), alternating-current output voltage (recorded on oscilloscope camera), direct-current bridge current, and bridge unbalance. Other information to be obtained should include the size of the bridge resistors and the cold resistance of each wire used. This information may then be used to compute magnitudes of blade wakes (see appendix E) if accuracies of ± 5 percent are adequate.

An oscillogram of several blade wakes in a centrifugal compressor is shown in figure 26. The evaluation of this trace is explained in appendix E.

Compressor surge and rotating stall. - The study of surge and rotating or propagating stall in compressors (reference 16) involves the

measurement of the frequency of the stall and the magnitude of the mass-flow changes. In these studies the mass-flow changes are large (over 100 percent) and periodic.

The apparatus connections are shown in figure 25(c). When the magnitude of the mass-flow changes is desired, the measurements are taken with the apparatus connected as in the study of velocity profiles (fig. 25(b)). The oscilloscope trace is photographed and then evaluated.

OF92

For the quantitative evaluation of the mass-flow changes, it is necessary to record (see equation (F5)) the values of the bridge current, the bridge arm resistance values, the "cold" resistance, the over-all gain of the system and, of course, a calibration curve. The calibration curves given with this report could be used if a ± 5 percent accuracy were sufficient. If not, then calibration curves would have to be run especially for the particular wires and testing apparatus in which they were to be used.

An oscillogram of two hot-wire traces resulting from rotating stall in a compressor is shown in figure 27. The two signals are not in phase, as is clearly seen from the photograph. The two probes were located in the same plane in the compressor but were separated by an angle which is related to the phase difference of the two signals. This is an indication that the stall region is rotating about the compressor.

Nonperiodic Phenomena

Intensity of turbulence. - The constant-current hot-wire anemometer has been used for a number of years to measure the intensity of turbulence. The equipment described in this report has been used for measurements of this type. Because of its relatively large input noise level (approximately 500 microvolts), it is not so useful in this case as the more conventional constant-current system. An effort is being made to reduce the input noise level.

The method of arranging the apparatus needed for intensity measurements is indicated in figure 25(d). The signal from the hot wire (the instantaneous bridge unbalance) is led directly to the average-square computer. This instrument gives a reading which is readily convertible to the intensity of turbulence. From the equation (see appendix F for derivation)

$$\frac{\Delta(\rho V)}{\rho v} = \frac{4}{\left[1 - \left(\frac{e_0}{\bar{e}_w}\right)^2\right]} \frac{\Delta e_w}{\bar{e}_w} \quad (6)$$

if the fluctuations in mass flow are small enough that

$$\frac{\Delta(\rho V)}{\Delta e_w} = \frac{\sqrt{\Delta(\rho V)^2}}{\sqrt{\Delta e_w^2}}$$

there results

$$\frac{\sqrt{\Delta(\rho V)^2}}{\rho V} = \frac{4}{\left[1 - \left(\frac{e_0}{e_w} \right)^2 \right]} \frac{\sqrt{\Delta e_w^2}}{\bar{e}_w} \quad (7)$$

where $\sqrt{\Delta e_w^2}$ is the reading of the average-square computer and $\sqrt{\Delta(\rho V)^2}/\rho V$ is the intensity of turbulence.

Spectrum of turbulence. - It is often desirable to determine the distribution of energy within a test installation as a function of frequency. Experience has shown that often large periodic fluctuations are present in the spectrum which are caused by ducting resonance and exhaust pulsations superimposed on the basic isotropic turbulence pattern. To determine the presence of these pulsations and the frequency associated with them is a primary function of the hot-wire anemometer. The diagrams of figures 25(e) and 25(f) show the connections to be made and the apparatus to be used for these measurements.

In the first method a variable low-pass electronic filter is used with the hot-wire anemometer and the average-square computer. As the upper cut-off frequency of the filter is increased, readings of the average-square computer are obtained which are proportional to the cumulative energy of the spectrum of turbulence. This spectrum can be interpreted by the method of Dryden (reference 14).

In the second method a variable-frequency band-pass wave analyzer is used with the hot-wire anemometer to obtain readings proportional to the energy of the spectrum in a narrow (5 cycles) band of frequencies. This method is particularly useful if periodic fluctuations are superimposed on the isotropic turbulence at certain frequencies.

Scale of turbulence. - Scale measurements are made by either of two methods: (a) Measurement of the correlation coefficient by means of two hot wires, or (b) measurement of longitudinal scale from the spectrum of turbulence.

The diagram of the equipment connections for the two-wire method is given in figure 25(g). The outputs of two hot wires are combined as indicated in appendix G to give the correlation coefficient. Two hot

wires are mounted parallel to each other on a special probe (fig. 28). By means of probe actuator motors, the distance between the parallel wires can be varied from nearly zero to approximately 2 inches. Each wire is controlled by a constant-temperature hot-wire anemometer amplifier and bridge. The outputs of the two wires (the instantaneous unbalances of the two bridges), after being initially equalized by means of the bridge resistance adjustment on the amplifier, are combined by the double-correlation circuit to give the lateral correlation coefficient. To determine the correlation coefficient from the reading of the ratio meter, use is made of the equation

$$\mathcal{R}_y = \frac{1 - r}{1 + r} \quad (G7)$$

The value of r is read from the ratio meter of the double-correlation instrument.

The procedure for measuring the longitudinal scale from the spectrum makes use of equation (5) if the cumulative energy spectrum is available or equation (6) if the energy spectrum at discrete frequencies has been determined.

Corrections to the measured scale are necessary for the effect of the finite length of the wire unless its magnitude is somewhat greater than the length of the wire. Schubauer (reference 13) gives a method for making this correction.

Empirical relations between the lateral and longitudinal scales and the Lagrangian scale can be used to obtain from the single-wire method the complete scale measurement.

Lewis Flight Propulsion Laboratory
National Advisory Committee for Aeronautics
Cleveland, Ohio, August 12, 1952

APPENDIX A

SYMBOLS

The following symbols are used in this report:

A,B,C,D,E,F	constants
d	wire diameter
e	instantaneous voltage, $\bar{e} + \Delta e$
\bar{e}	average value of voltage
e_0^2	$RA(R - R_a)$
f(e)	function of e
I	current (direct-current component)
i	instantaneous current
\bar{i}	average value of current
K	calibration constant (gain of anemometer)
k	thermal conductivity of air
L	scale of turbulence
l	length of wire
M	Mach number
Nu	Nusselt number
n	frequency
Pr	Prandtl number
p	pressure
R	resistance of hot wire
α	correlation coefficient
Re	Reynolds number
r	reading of ratio meter on double-correlation computer

2640

S	cross-sectional area of wire
t	temperature
Δt	$t_w - t_r$
U	mean flow velocity
u	velocity fluctuation component in x-direction
$\sqrt{u^2}$	root mean square of u
v	velocity fluctuation component in y-direction
w	velocity fluctuation component in z-direction
x,y,z	a right-hand Cartesian coordinate system with x in direction of stream flow
α	temperature coefficient of resistance
μ	coefficient of viscosity of air
ρ	density of air
$\rho^* a^*$	critical mass flow
ρV	instantaneous mass flow, $\bar{\rho} \bar{V} + \Delta(\rho V)$
$\bar{\rho} \bar{V}$	mass flow as determined by \bar{e} and calibration curve
$\rho_0 V_0$	A^2/B^2
σ	resistivity of wire material

Subscripts:

0	reference conditions
a	conditions at a
b	conditions at bridge
f	value computed at film temperature, $t_f = \frac{t_w + t_r}{2}$
g	conditions of bridge galvanometer

h upper cut of point
n frequency
p conditions at vacuum tube plate
r recovery conditions
s static conditions
t total conditions
w wire
x lateral direction
y longitudinal direction

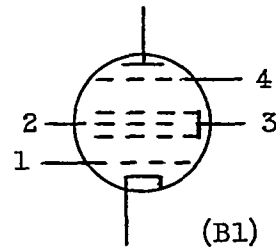
2640

APPENDIX B

THEORY OF AVERAGE-SQUARE COMPUTER

The current for a multielectrode tube as shown in the sketch may be represented by the equation

$$i_p = Ce_1 + De_1e_2 \cos \theta_{1-2} + Ee_2 + F$$



(Grids 1 and 2 are biased negative to cathode, grid 3 is held positive at a fixed value, grid 4 is returned to the cathode, and subscripts refer to grid numbers.)

The only alternating-current components are Ce_1 and Ee_2 . The component of plate current as read by a direct-current meter therefore is

$$I_p = De_1e_2 \cos \theta_{1-2} + F \quad (B2)$$

When two tubes with their plates connected for push-pull operation and their grids phased as indicated in figure 9 are used, the plate current in the first tube will be

$$I_{p,1} = De_1e_2 \cos 0^\circ + F \quad (B3)$$

and in the second,

$$I_{p,2} = -(De_1e_2 \cos 180^\circ + F) \quad (B4)$$

and

$$I_{p,1} + I_{p,2} = De_1e_2 \cos 0^\circ + F - De_1e_2 \cos 180^\circ - F = 2 De_1e_2 \quad (B5)$$

Since $|e_1| = |e_2|$,

$$I_{p,1} + I_{p,2} = 2 De_1^2 \quad (B6)$$

Resistance-capacitance network in the output circuit averages this current so that the final meter reading is $2De_1^2$.

APPENDIX C

OPERATION INSTRUCTIONS

Constant-Temperature Hot-Wire Anemometer

The following operating instructions apply to the constant-temperature hot-wire anemometer shown in figure 1. The bridge (fig. 5) is connected as shown in figure 29. Before the power switch is turned on, a check should be made that the switches controlling the galvanometer, the grids, and the output are in the neutral or "no connection" position.

- (1) Turn on the power switch and wait for the unit to warm up (three pilot lights are lighted).
- (2) Turn the bridge resistance control to zero resistance.
- (3) Turn the bridge current controls to their minimum current setting.
- (4) Set switches as follows:
 - (a) galvanometer sensitivity to high
 - (b) grids to input
 - (c) output to "on" position
- (5) Balance the bridge.
 - (a) Adjust the bridge current controls (fine and coarse) until the bridge current meter indicates a small flow of current. The galvanometer should show an unbalance current greater than 10 microamperes.
 - (b) Adjust the bridge resistance control slowly and carefully (especially during the initial turns) until its resistance is a maximum.
 - (c) Adjust the fine current control for a bridge unbalance current of not less than 2 microamperes.

The hot-wire anemometer is now ready for operation and a minimum of attention is needed during a run. The bridge unbalance should be checked periodically during the run. More adjustments will be required during the first few minutes of operation when the amplifier has not had time to warm up completely.

Average-Square Computer

The operating instructions for the average-square computer shown in figure 30 are as follows:

- (1) Turn on the power switch and wait approximately 1 minute for the unit to warm up.
- (2) Turn the zero adjust control to set the output meter to zero.
- (3) Set the range selector switch to least gain ($\times 10,000$).
- (4) Connect a signal to the input terminal.
- (5) Rotate the range selector switch until a reading less than one-tenth of full scale is obtained.
- (6) Push the "press-to-read" switch to obtain the output meter reading.

The output meter reading is multiplied by the range selector value and referred to figure 12 to determine the root-mean-square value of the input signal.

Auxiliary Current Supply

The auxiliary current supply shown in figures 13 and 31 is operated as follows:

- (1) Connect the output of the anemometer to the input of the auxiliary current supply.
- (2) Connect the output of the auxiliary current supply to the bridge input.
- (3) Put the anemometer into operation in the usual manner except for the part on adjusting the bridge resistance control.
- (4) Adjust the bridge resistance control until the bridge current is approximately two-thirds of the maximum current available.
- (5) Adjust the coarse current control on the auxiliary supply until the bridge current supplied by the anemometer is reduced to approximately one-third of the maximum current available.
- (6) Repeat steps 4 and 5 until the bridge resistance control is at its maximum value.

(7) Adjust the fine current control on the auxiliary current supply until the anemometer bridge current is approximately one half of the maximum available current supply.

(8) Continue with anemometer adjustments, step (7c).

For shutdown, remove the wire from the anemometer heating circuit in the usual way and reduce the auxiliary current to zero with the coarse current control.

2640

Double-Correlation Computer

The double-correlation computer of figure 32 is operated as follows:

(1) Place the two hot wires whose signals are to be correlated in close proximity in the air stream.

(2) Adjust the bridge resistance control on the anemometer with the largest output signal until the two anemometer outputs are equal as read on average-square computers.

(3) Connect the two anemometer outputs to the inputs of the correlation instrument.

(4) Connect cables between the double-correlation instrument and two average-square computers as shown in figure 33.

(5) Adjust the average-square computers in the usual way.

The reading of the ratio meter may be used in equation (G7) to obtain the correlation coefficient.

APPENDIX D

CALIBRATION OF ELECTRONIC EQUIPMENT

If the voltage output from the bridge is to be determined while operating, it is necessary to determine the gain of the over-all instrumentation from bridge to final recorder or oscilloscope. An audio signal generator may be used to inject a signal into the system at the bridge input. The amplitude of the input signal should be adjusted to give a normal reading on the recorder (1 or 2 in.). The input signal should now be read with a vacuum tube voltmeter. The over-all sensitivity may be determined by dividing the input signal by the output deflection. This quotient gives the voltage required at the input to give 1 inch deflection at the output. Of course, this calibration would change for every setting of the recorder gain control or if other elements were introduced, such as filters or decade amplifiers. If the data are photographed, it is also necessary to know the magnification factor for the camera as used.

260

APPENDIX E

REDUCTION OF DATA

Mean Flow Calibration

Two types of mean flow calibration curve have proved useful and the method of obtaining each will be presented. These are:

$$(1) \text{ A graph of } \frac{\bar{i}_w^2 R_w}{R_w - R_{w,a}} \text{ against } \sqrt{\rho V}$$

$$(2) \text{ A graph of } Nu_f / Pr_f^{0.3} \text{ against } \sqrt{Re}$$

The first of these is the type of calibration needed to reduce fluctuation data from voltage fluctuations to mass-flow fluctuations. In this case, since the calibration conditions are as nearly identical to the test conditions as possible, no corrections are made for loss of heat by the wire through conduction to the prongs. The essential data required in this calibration are the following:

- (1) The wire current or the bridge current (with no air flow; with flow)
- (2) The operating resistance of the wire
- (3) The "cold" resistance of the wire (by "cold" resistance is meant the resistance of the unheated wire at some known temperature t_a)
- (4) The Mach number (to be held constant)
- (5) The total pressure in the plenum chamber
- (6) The total temperature in the plenum chamber
- (7) The dynamic pressure (total pressure minus static pressure) required to keep the Mach number constant
- (8) The bridge unbalance current

For a constant Mach number it has been found convenient to set the dynamic pressures corresponding to a series of total pressures that are

2640

perfect squares (in any units whatsoever) and determine the wire current necessary to balance the bridge at each setting. A plot of \bar{I}_w^2 against $\sqrt{p_t}$ should result in a straight line (approximately) and serves as a rough check on the final calibration. From this data it is possible to calculate the heat loss from the wire and the mass flow past the wire. For example, a typical set of data taken with the constant-temperature hot-wire anemometer can be evaluated as follows. The data are

Bridge current \bar{i}_b

Bridge unbalance current \bar{i}_g

Operating resistances of bridge R_1 , R_3 , and R_4

"Cold" resistance $R_{w,a}$

Mach number M

Total pressure p_t

Dynamic pressure $p_t - p_s$

Total temperature t_t

Use is made of the following relations to calculate the operating resistance of the wire and the wire current:

$$R_w = \frac{(R_1 + R_3)(R_4 \bar{i}_b + R_g \bar{i}_g)}{R_3 \bar{i}_b - (R_g + R_1 + R_3) \bar{i}_g} - R_4 \quad (E1)$$

$$\bar{i}_w = \bar{i}_b \frac{R_3 + R_4}{R_1 + R_w + R_3 + R_4} \quad (E2)$$

The values of $\rho V / \rho^* a^*$ for various Mach numbers are given in reference 17 and hence ρV can be calculated. These calculations give the coordinates of points of the calibration curve.

If the more general calibration curve involving nondimensional parameters is desired, it is necessary to continue the calculations. The Reynolds number can be obtained from the mass flow by means of the equation

$$Re = \frac{\rho V d}{\mu} \quad (E3)$$

The value of μ (the viscosity of air) is obtained from tables of the National Bureau of Standards (reference 18) which give the values of the viscosity as a function of temperature. The temperature used in this report is the film temperature defined in appendix A. Other observers, however, have used the total temperature as the desired temperature for evaluating the viscosity.

The Nusselt number can be calculated by means of the equation

$$Nu = \frac{\frac{l^2 R_w}{\pi k l (t_w - t_r)}}{=} \frac{\frac{l^2 R_w}{\pi k l \Delta T}}{} \quad (E4)$$

The value of k (the thermal conductivity of air) is obtained from tables of reference 19 and the temperature used is the film temperature as is the case for the viscosity. The length of the wire l is the length of the unplated section of the tungsten wire and is measured by a measuring microscope at the time the wire is mounted. The temperature of the wire is calculated as follows:

$$R_{w,a} = R_0 [1 + \alpha(t_a - 32^\circ)]$$

$$R_w = R_0 [1 + \alpha(t_w - 32^\circ)] \quad (E5)$$

$$t_w = \frac{(R_w - R_{w,a})(1 - 32\alpha) + R_w \alpha t_a}{\alpha R_{w,a}}$$

Now, since $\Delta t = t_w - t_r$ and t_r can be obtained from temperature recovery data (see, for example, reference 7, fig. 18), the Nusselt number can be readily calculated. If the Nusselt numbers are to be corrected for end-loss effects, the calculation is an involved one given in reference 7 or is a somewhat simpler method found in reference 12, which gives comparable end corrections.

In most of the measurements of fluctuations in mass flow, end-loss corrections are unnecessary because the calibration and use conditions of the wires are essentially the same and the fluctuations are expressed in parameters which are unaffected by the end losses.

Fluctuation calibration. - In many of the situations met in measurements of fluctuating flows, the record consists of a photograph of an oscilloscope trace. The direct problem thus becomes a transformation of the voltage fluctuations as a function of time into a mass-flow fluctuation with respect to time. The required data in this case are the same as outlined plus the photograph of the trace on the cathode-ray tube.

2540

An example of such a trace is given in figure 26. In order to evaluate this trace some additional information is desirable. A mean flow line around which the fluctuations take place and the magnification factors of the camera and enlarger are essential if quantitative results are desired. The mean flow line can usually be obtained on the face of the oscilloscope by reducing the gain enough to give a mean line trace. A second and generally more satisfactory way is illustrated by figure 26(b). In this figure the mean flow line has been obtained by finding the area between the curve and a horizontal line through the lowest ordinate on the curve. The mean line is drawn at a distance above this horizontal line equal in units to the area under the curve divided by the time elapsed for the record.

When this mean flow line has been obtained the values of Δe_w can be measured above or below this line and can be substituted in equation (F5) or (F7), depending on whether the values of Δe_w are small or large, respectively, compared with the value of the voltage corresponding to the mean flow, to give the mass-flow fluctuations.

The evaluation of the oscillogram shown in figure 25(a), which represents the mass-flow profile between adjacent blade wakes of a 48-inch compressor 1/2 inch beyond the impeller tip measured at a station 0.1 inch from the rear diffuser wall, is obtained as follows. The data are

Bridge current (with no flow) $\bar{i}_{b,0}$

Bridge unbalance current \bar{i}_g

Operating resistances of bridge R_1 , R_3 , and R_4

"Cold" resistance of wire $R_{w,a}$

Bridge current (with flow) \bar{i}_b

Mach number M

Over-all gain of hot-wire equipment K (see appendix D)

The wire current \bar{i}_w and the actual wire resistance R_w are calculated as explained for the mean flow calibration. To calculate the Nusselt number, it is necessary to find the wire temperature, the film temperature, and, finally, the temperature difference between the wire and the air stream.

With this value of the Nusselt number, the Prandtl number calculated at the film temperature, and the calibration curve given with this report (see fig. 34), the Reynolds number corresponding to the flow can be

calculated. Figure 34 gives average calibration curves of a hot wire of $l/d = 400$ with end corrections. Obtaining the mass flow from the Reynolds number is an easy calculation.

Now, if

$$\bar{i}_{w,0} = \bar{i}_{b,0} \frac{R_3 + R_4}{R_1 + R_w + R_3 + R_4}$$

and

$$\bar{e}_0 = \bar{i}_{w,0} \times R_w$$

are calculated, it is possible to obtain the value of the mass-flow fluctuations by use of equation (F5) or (F7).

APPENDIX F

DERIVATION OF EQUATION FOR INTENSITY

The King equation (reference 20) describes the relation between the heat generated in a hot wire and the heat lost by forced convection to the air stream in which the wire is placed. This equation (derived ignoring the Mach number)

$$\frac{\bar{I}_w^2 R_w}{R_w - R_{w,a}} = A + B \sqrt{\rho V} \quad (F1)$$

is rewritten as

$$\left(\frac{e_w}{e_0}\right)^2 = 1 + \sqrt{\frac{\rho V}{\rho_0 V_0}} \quad (F2)$$

from which

$$\rho V = \rho_0 V_0 \left[\left(\frac{e_w}{e_0} \right)^2 - 1 \right]^2 \quad (F3)$$

is obtained. Since $\rho V = f(e)$,

$$\frac{f(\bar{e}_w + \Delta e_w) - f(\bar{e}_w)}{f(\bar{e}_w)} = \frac{\left[\left(\frac{\bar{e}_w + \Delta e_w}{e_0} \right)^2 - 1 \right]^2 - \left[\left(\frac{\bar{e}_w}{e_0} \right)^2 - 1 \right]^2}{\left[\left(\frac{\bar{e}_w}{e_0} \right)^2 - 1 \right]^2} \quad (F4)$$

After simplification and substitution of $\Delta(\rho V)/\rho V$ for $\frac{f(\bar{e}_w + \Delta e_w) - f(\bar{e}_w)}{f(\bar{e}_w)}$, this equation becomes

$$\frac{\Delta(\rho V)}{\rho V} = \frac{1}{\left[1 - \left(\frac{e_0}{\bar{e}_w} \right)^2 \right]} \left[\frac{4 \Delta e_w}{\bar{e}_w} + 2 \left(\frac{\Delta e_w}{\bar{e}_w} \right)^2 \right] + \frac{1}{\left[1 - \left(\frac{e_0}{\bar{e}_w} \right)^2 \right]^2} \left[4 \left(\frac{\Delta e_w}{\bar{e}_w} \right)^2 + 4 \left(\frac{\Delta e_w}{\bar{e}_w} \right)^3 + \left(\frac{\Delta e_w}{\bar{e}_w} \right)^4 \right] \quad (F5)$$

This expression reduces to the following when second and higher powers of Δe can be neglected:

$$\frac{\Delta(\rho V)}{\rho \bar{V}} = \frac{1}{\left[1 - \left(\frac{e_0}{e_w} \right)^2 \right]} \left(4 \frac{\Delta e_w}{e_w} \right) \quad (F6)$$

or

$$\frac{\Delta(\rho V)}{\rho \bar{V}} = \frac{4 \bar{e}_w \Delta e_w}{e_w^2 - e_0^2} \quad (F7)$$

APPENDIX G

MEASUREMENT OF CORRELATION COEFFICIENT AND SCALE

OF TURBULENCE BY TWO-WIRE METHOD

Let $e_{w,1}$ and $e_{w,2}$ be the voltage signals from two parallel hot wires separated by a distance y in an air stream where the velocity fluctuations are u_1 and u_2 . If these voltage signals are combined by addition and subtraction to obtain $(e_{w,1} + e_{w,2})$ and $(e_{w,1} - e_{w,2})$ and these results are fed into two average-square computers, there result $\overline{(e_{w,1} - e_{w,2})^2}$ and $\overline{(e_{w,1} + e_{w,2})^2}$. If these readings are now added and subtracted, the result is

$$\overline{(e_{w,1} - e_{w,2})^2} + \overline{(e_{w,1} + e_{w,2})^2} = 2\overline{e_{w,1}^2} + 2\overline{e_{w,2}^2} \quad (G1)$$

$$\overline{(e_{w,1} - e_{w,2})^2} - \overline{(e_{w,1} + e_{w,2})^2} = 2\overline{e_{w,1}e_{w,2}} \quad (G2)$$

$$\frac{\overline{(e_{w,1} - e_{w,2})^2} - \overline{(e_{w,1} + e_{w,2})^2}}{\overline{(e_{w,1} - e_{w,2})^2} + \overline{(e_{w,1} + e_{w,2})^2}} = \frac{2\overline{e_{w,1}e_{w,2}}}{\overline{e_{w,1}^2} + \overline{e_{w,2}^2}} \quad (G3)$$

But if the turbulence is uniformly distributed and isotropic so that the average square of the fluctuations is the same and if the hot wires are carefully matched as to output,

$$\frac{\overline{(e_{w,2} - e_{w,2})^2} - \overline{(e_{w,1} + e_{w,2})^2}}{\overline{(e_{w,1} - e_{w,2})^2} + \overline{(e_{w,1} + e_{w,2})^2}} = \frac{2\overline{e_{w,1}e_{w,2}}}{2\overline{e_w^2}} \quad (G4)$$

$$1 - \frac{\frac{\overline{(e_{w,1} + e_{w,2})^2}}{\overline{(e_{w,1} - e_{w,2})^2}}}{\frac{\overline{(e_{w,1} + e_{w,2})^2}}{\overline{(e_{w,1} - e_{w,2})^2}}} = \frac{\overline{e_{w,1}e_{w,2}}}{\overline{e_w^2}} \quad (G5)$$

$$\frac{1 - r}{1 + r} = \frac{\overline{e_{w,1} e_{w,2}}}{\sqrt{\overline{e_{w,1}^2}} \sqrt{\overline{e_{w,2}^2}}} \quad (G6)$$

Since the correlation coefficient is defined by the right-hand member of this equation,

$$\rho_y = \frac{1 - r}{1 + r} \quad (G7)$$

The scale of homogeneous turbulence is then found by the definition given previously.

2640

REFERENCES

1. Weske, John R.: A Hot-Wire Circuit with Very Small Time Lag. NACA TN 881, 1943.
2. Ossofsky, Eli: Constant Temperature Operation of the Hot-Wire Anemometer at High Frequency. Rev. Sci. Instr., vol. 19, no. 12, Dec. 1948.
3. Kovasznay, Leslie S. G.: Simple Analysis of the Constant Temperature Feedback Hot-Wire Anemometer. Aero/JHU CM-478, Dept. Aero., Johns Hopkins Univ., June 1, 1948. (NOrd-8036, T.O. JHB-6.)
4. Taylor, G. I.: Diffusion by Continuous Movements. Proc. London Math. Soc., vol. 20, 1922, pp. 196-212.
5. Scadron, Marvin D., and Warshawsky, Isidore: Experimental Determination of Time Constants and Nusselt Numbers for Bare-Wire Thermocouples in High-Velocity Air Streams and Analytic Approximation of Conduction and Radiation Errors. NACA TN 2599, 1952.
6. Pierce, John R.: A Proposed Wattmeter Using Multielectrode Tubes. Proc. Inst. Rad. Eng., vol. 24, no. 4, April 1936, pp. 577-583.
7. Lowell, Herman H.: Design and Application of Hot-Wire Anemometers for Steady-State Measurements at Transonic and Supersonic Airspeeds. NACA TN 2117, 1950.
8. McAdams, William H.: Heat Transmission. 2d ed., McGraw-Hill Book Co., Inc. (New York and London), 1942.
9. Schubauer, G. B., and Klebanoff, P. S.: Theory and Application of Hot-Wire Instruments in the Investigation of Turbulent Boundary Layers. NACA ACR 5K27, 1946.

- 2640
10. Strehlow, Roger A.: A Method for Electroplating Fine Wires. Univ. Wisconsin, CM-551, June 27, 1949. (Navy BuOrd Contract NOrd 9938, Task WIS-1-E.)
 11. Colner, William H., Feinleib, Morris, and Francis, Howard T.: Preparation of Very Fine Wire by Electropolishing. Metal Progress, vol. 59, no. 6, June 1951, pp. 795-797.
 12. Kovasznay, Leslie S. G., and Törmärck, Sven I.. A.: Heat Loss of Hot-Wires in Supersonic Flow. Bumblebee Series, Rep. No. 127, Johns Hopkins Univ., Dept. Aero., April 1950. (Contract NOrd 8036, with Bur. Ordnance, U. S. Navy.)
 13. Dryden, Hugh L., Schubauer, G. B., Mock, W. C., Jr., and Skramstad, H. K.: Measurements of Intensity and Scale of Wind-Tunnel Turbulence and Their Relation to the Critical Reynolds Number of Spheres. NACA Rep. 581, 1937.
 14. Dryden, Hugh L.: A Review of the Statistical Theory of Turbulence. Quarterly Appl. Math. vol. I, no. I, April 1943, pp. 7-42.
 15. Younger, George G., Gabriel, David S., and Mickelsen, William R.: Experimental Study of Isothermal Wake-Flow Characteristics of Various Flame-Holder Shapes. NACA RM E51K07, 1952.
 16. Grant, Howard P.: Hot Wire Measurements of Stall Propagation and Pulsating Flow in an Axial Flow Inducer-Centrifugal Impeller System. Pratt and Whitney Res. Rep. No. 133, June 1951.
 17. Emmons, Howard W.: Gas Dynamics Tables for Air. Dover Pub., Inc. (N. Y.), 1947.
 18. Anon.: The NBS-NACA Tables of Thermal Properties of Gases. Table 2.39-Dry Air; Coefficients of Viscosity. Nat. Bur. Standards, Dec. 1950.
 19. Anon.: The NBS-NACA Tables of Thermal Properties of Gases. Table 2.42-Dry Air; Thermal Conductivity. Nat. Bur. Standards, Dec. 1950.
 20. King, Louis Vessot: On the Convection of Heat from Small Cylinders in a Stream of Fluid: Determination of the Convection Constants of Small Platinum Wires with Applications to Hot-Wire Anemometry. Proc. Roy. Soc. (London), vol. 214, no. 14, ser. A, Nov. 1914, pp. 373-432.

TABLE I - HOT-WIRE MATERIALS RATED ACCORDING TO SOME DESIRABLE
PHYSICAL PROPERTIES AND AVAILABILITY

[The numbers indicate grades of decreasing quality
with number 1 being best.]



Material	Temperature coefficient of resistance	Tensile strength	Ability to resist oxidation	Time constant	Availability
Tungsten	2	1	4	1	1
Platinum	3	4	1	3	2
Nickel	1	3	3	4	4
Platinum-iridium (80 percent platinum)	4	2	2	2	3

TABLE II - COMPARISON OF WIRE DIAMETERS OBTAINED BY THREE
DIFFERENT METHODS

Wire material	Diameter			
	Nominal	Measured by method A ¹	Measured by method B ²	Measured by method C ³
Tungsten	0.0002	0.0002(1±0.10)	0.000248(1±0.02)	-----
	.000125	.00013(1±0.10)	-----	-----
	.00014	-----	0.000181(1±0.02)	-----
Platinum-iridium (80 percent platinum)	.0004	-----	-----	-----
	.0008	.00083(1±0.02)	-----	0.00085(1±0.05)
	.001	.001(1±0.02)	-----	.00115(1±0.05)

¹Calculated from resistance of a measured length.

²Measurement of a diameter from electron micrograph.

³Measuring microscope.

TABLE III - COMPARABILITY OF HOT-WIRE ANEMOMETER PROBES



Probe	R_0 (Ω) before calibration	R_0 (Ω) after calibration	Change ^a (percent)
125	6.564	6.750	2.8
129	6.420	6.567	2.2
130	6.473	6.593	1.8
130 ^b	6.427	6.463	.5
130 ^c	6.463	6.463	0
125 ^b	6.192	6.192	0
127	6.465	6.571	1.6
125 ^c	6.192	6.192	0

^aDue to an initial annealing during the first few minutes after operation; subsequent runs with the same wire show no further change.

^bProbe destroyed and rewired.

^cRerun.

2640

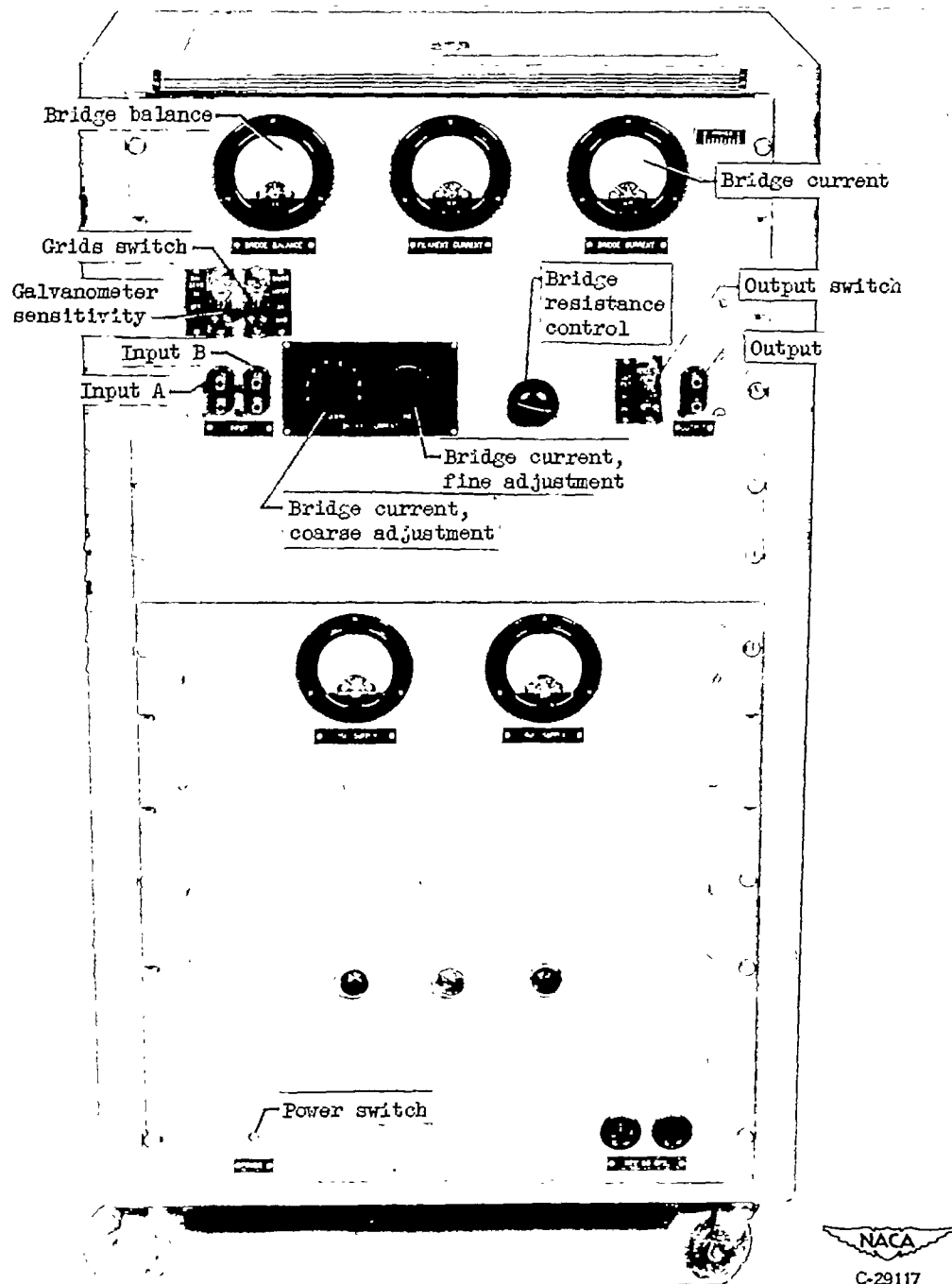
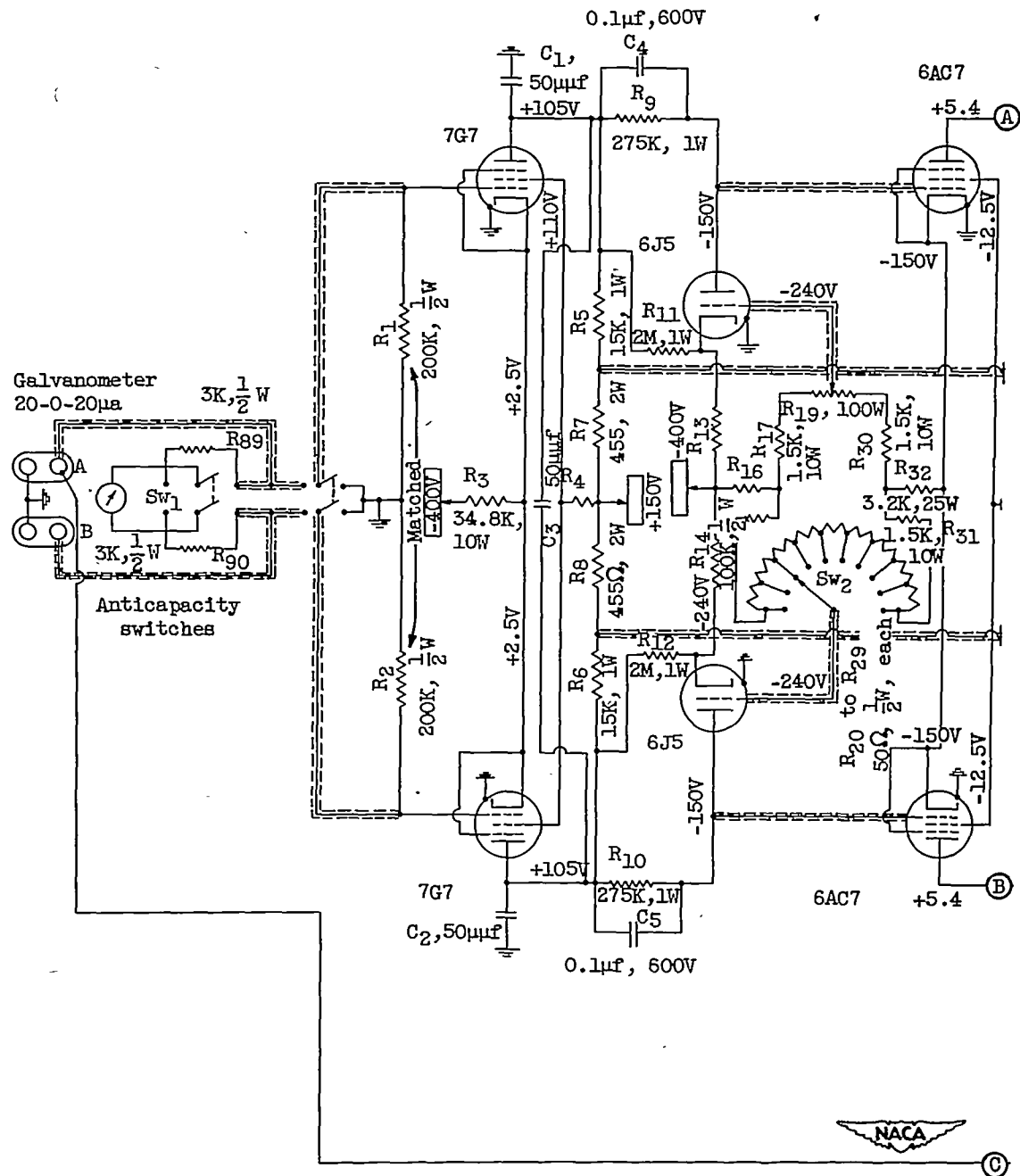


Figure 1. - Constant-temperature hot-wire anemometer amplifier.

C-29117



2640

41

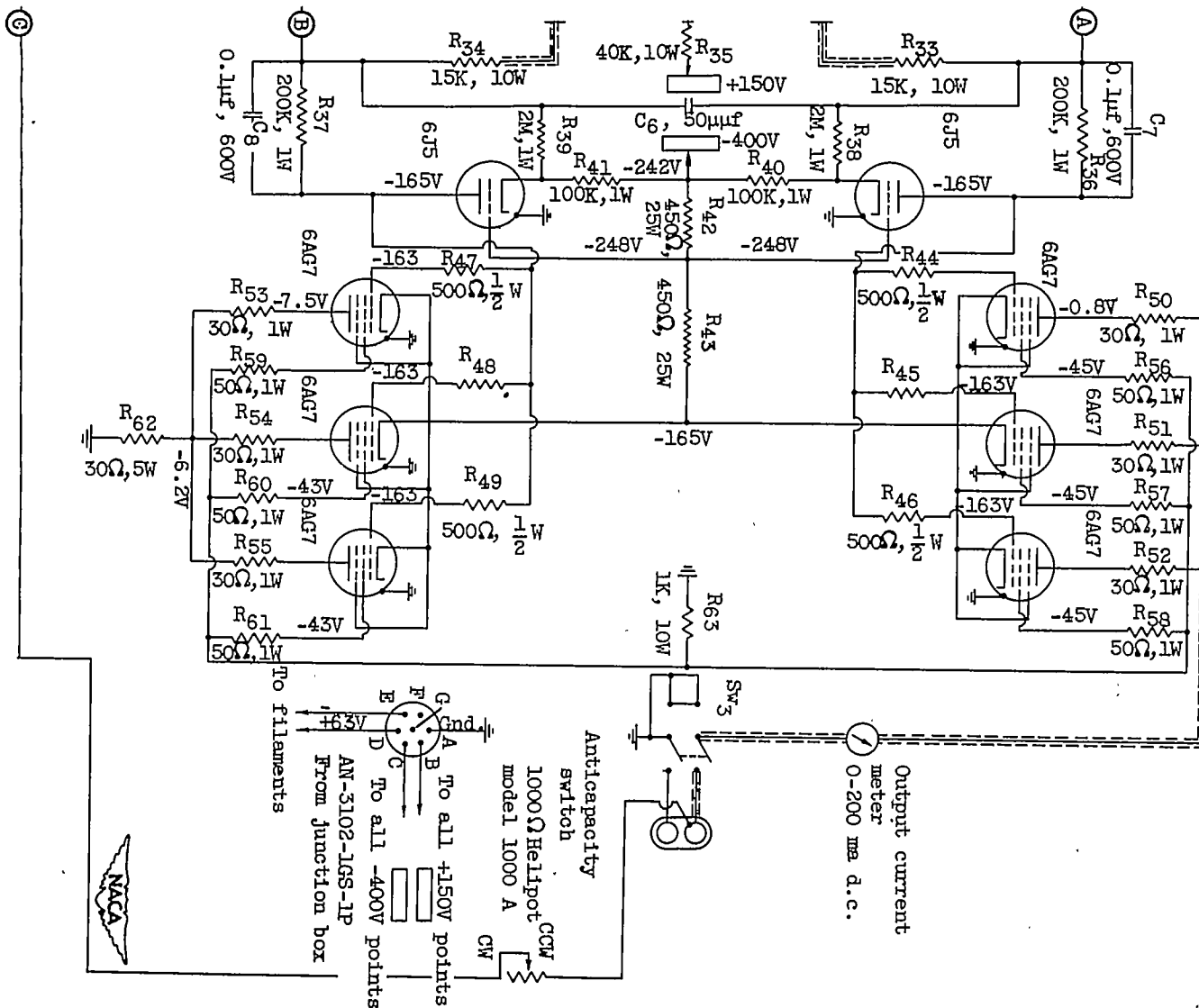
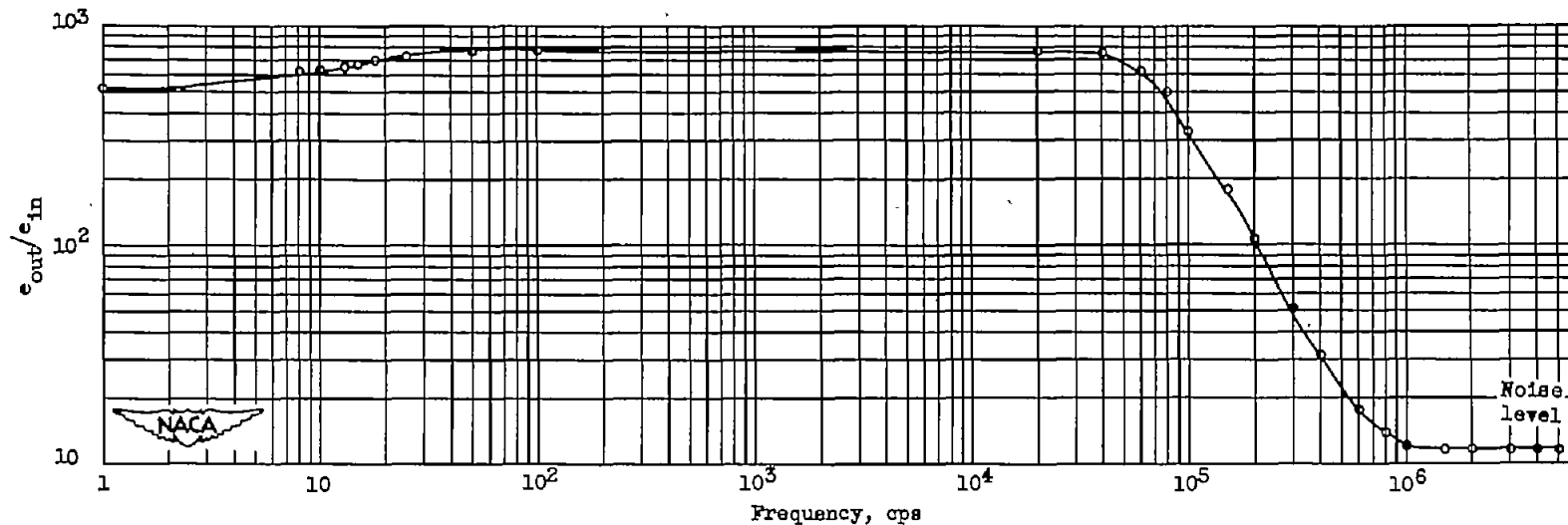


Figure 2. - Hot-wire anemometer with d-c amplifier.



A-c response measurements

Input	0.002V
External load	50Ω
Output current	80ma
Input circuit	One grid grounded, signal between other grid and ground

D-c response measurements

Input	0.001mV
External load	50Ω
Output current	80ma (0 signal)
Input circuit	Same as for a-c measurements
Output voltage at 0 signal	4.36V
Output voltage at 0.001V signal	3.84V
D-c gain	520

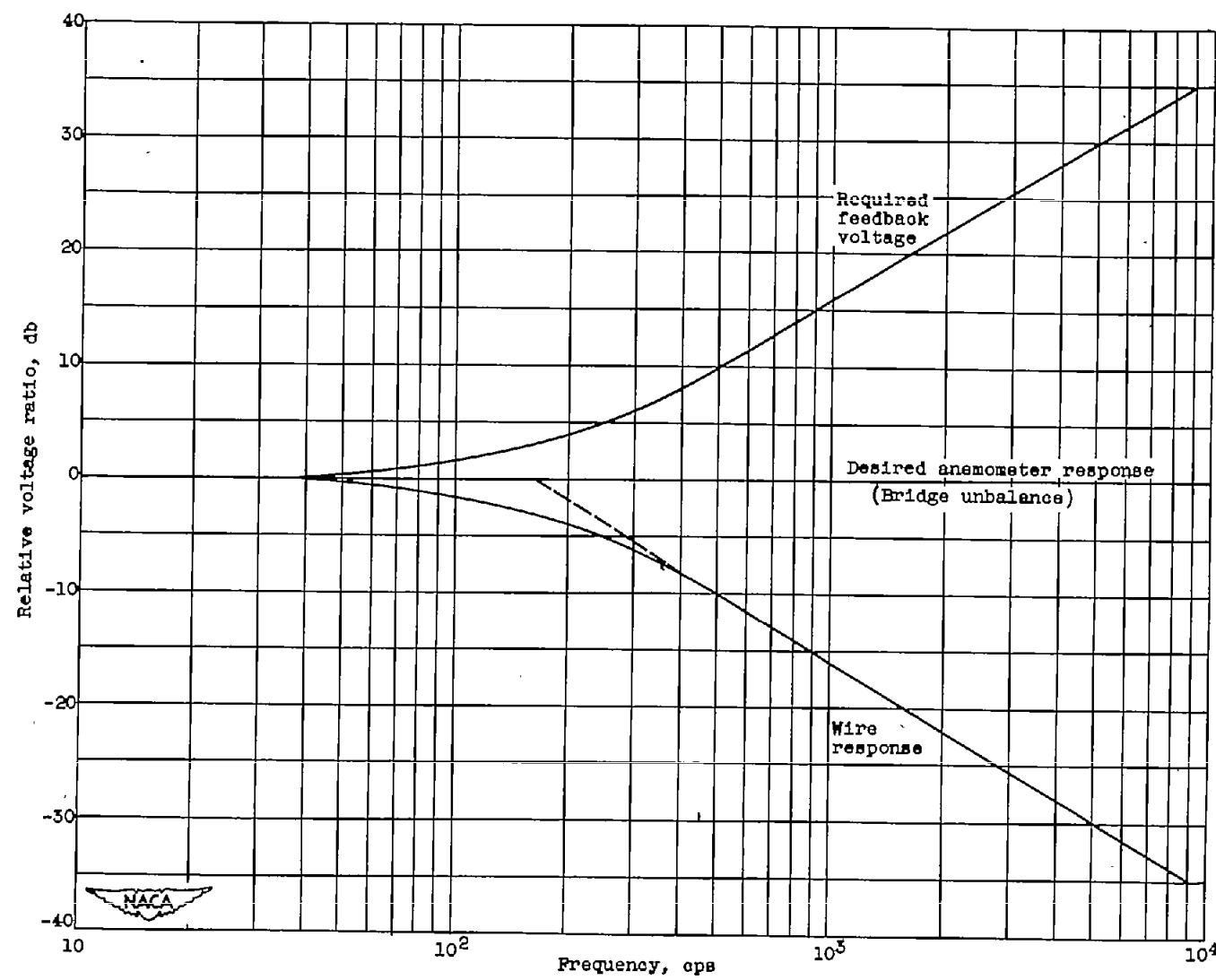


Figure 4. - Theoretical frequency response.

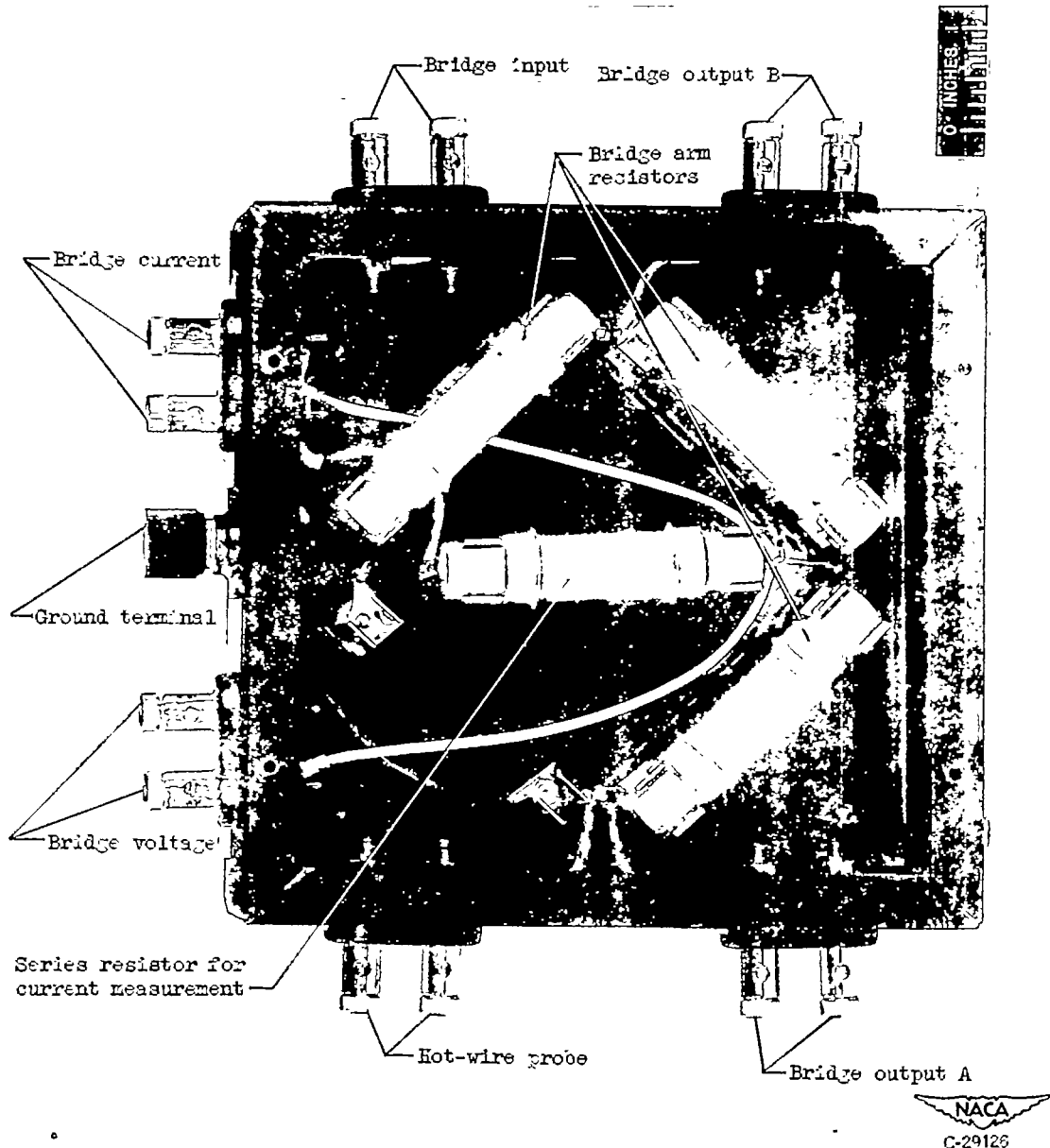


Figure 5. - Hot-wire bridge.

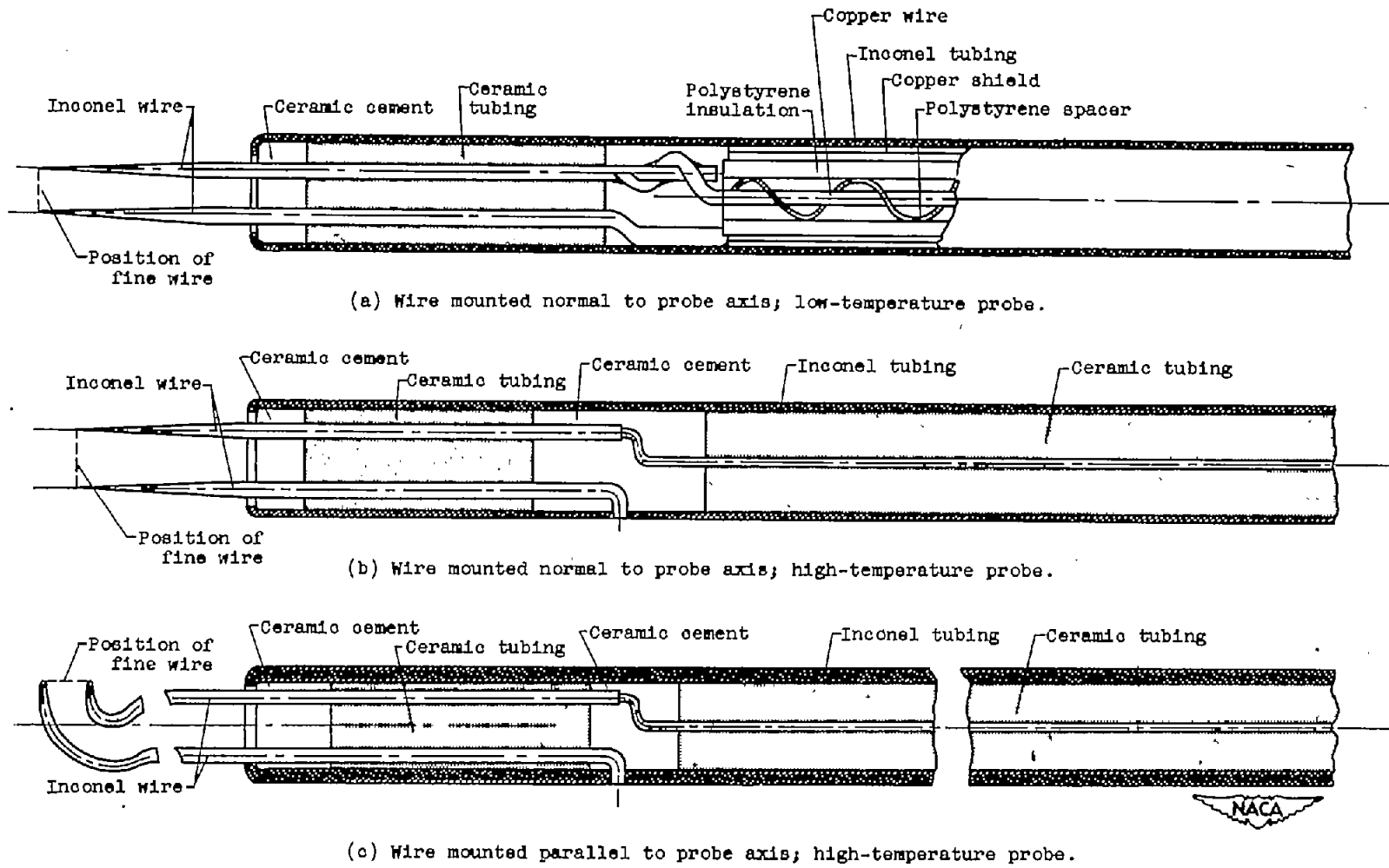


Figure 6. - Hot-wire anemometer probes.

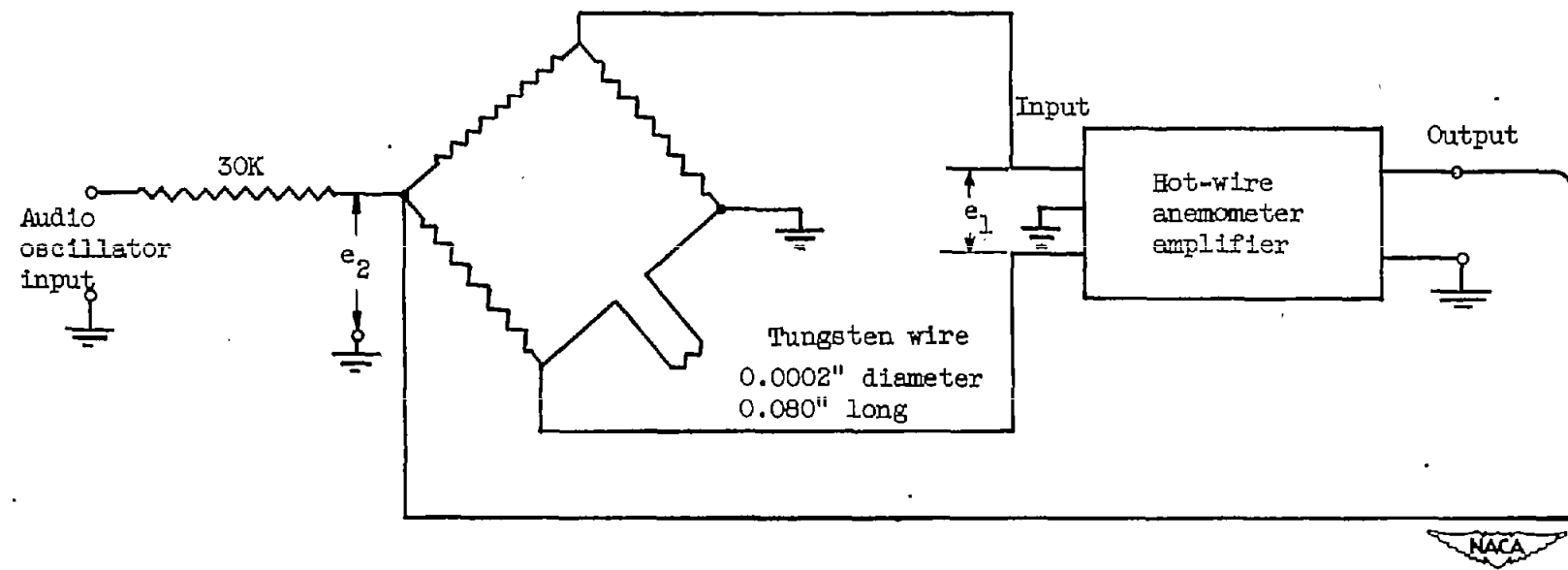


Figure 7. - Diagram for frequency-response measurements of hot-wire anemometer.

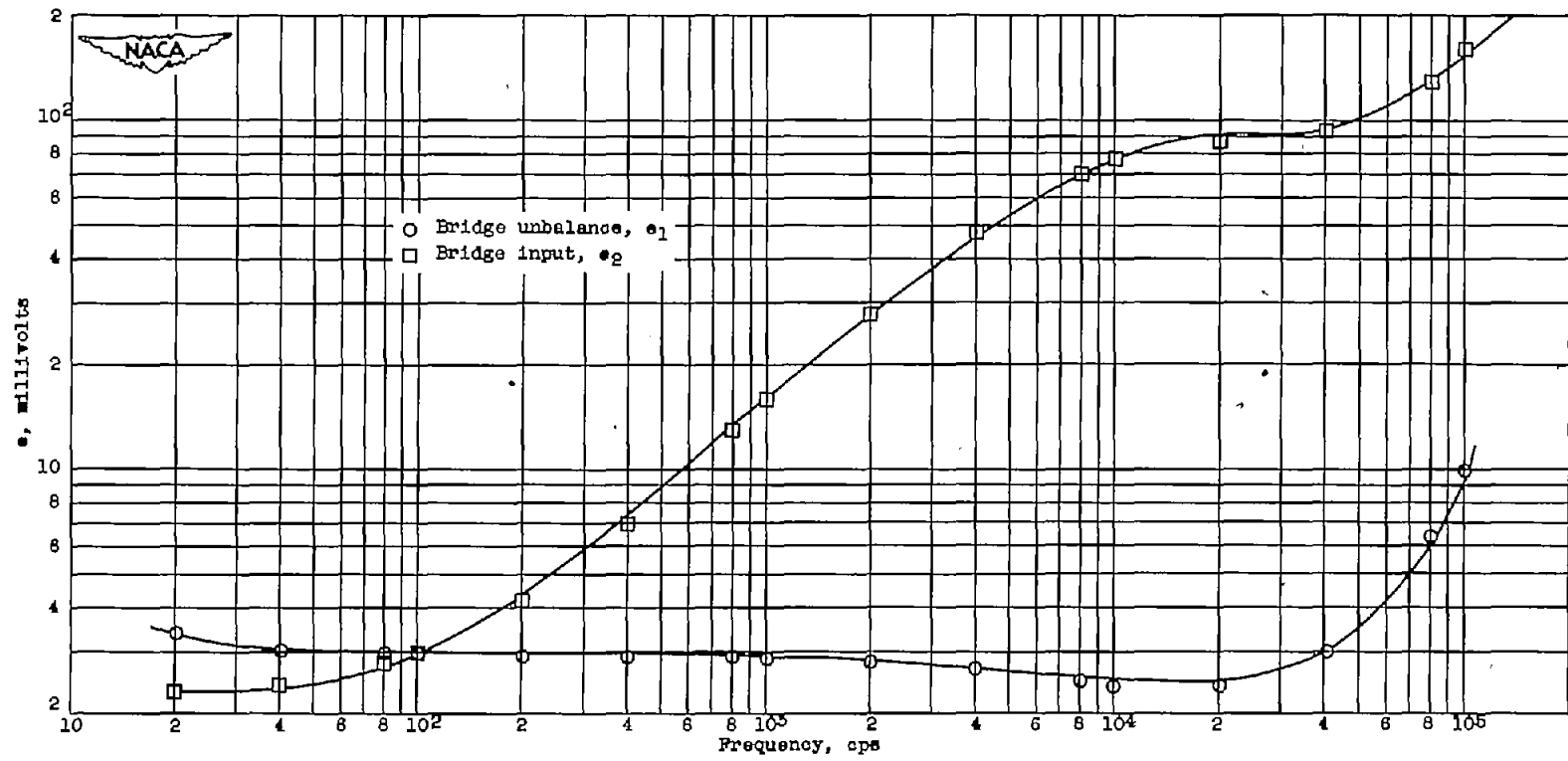


Figure 8. - Response curves of constant-temperature hot-wire anemometer; wire diameter, 0.0002 inch; length, 0.080 inch.

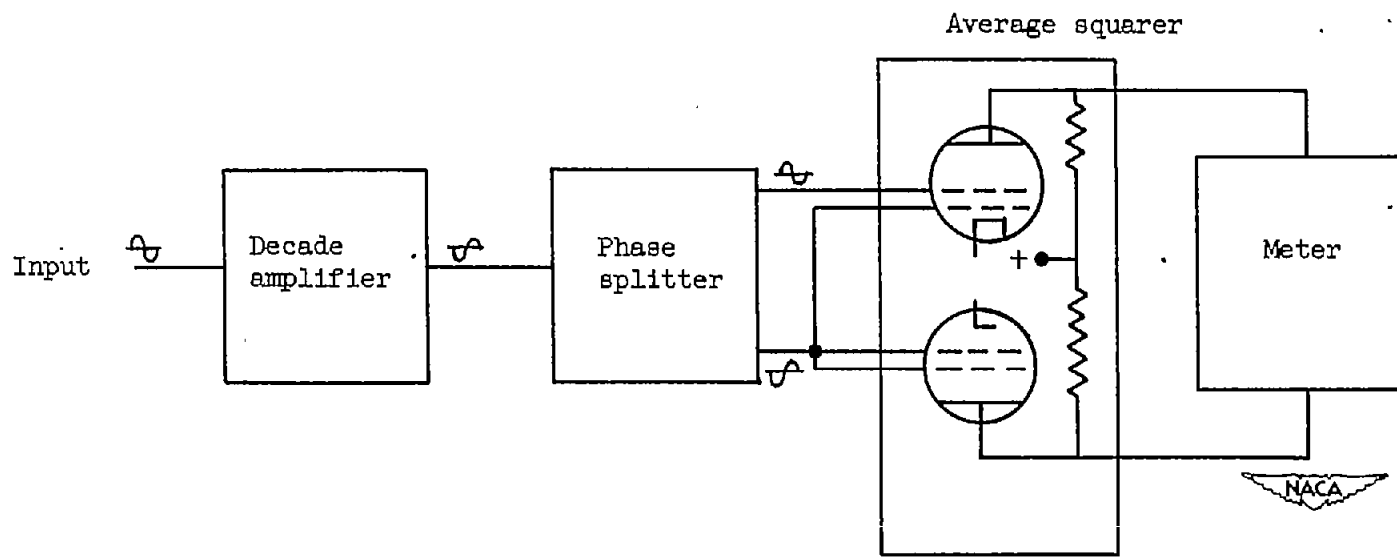
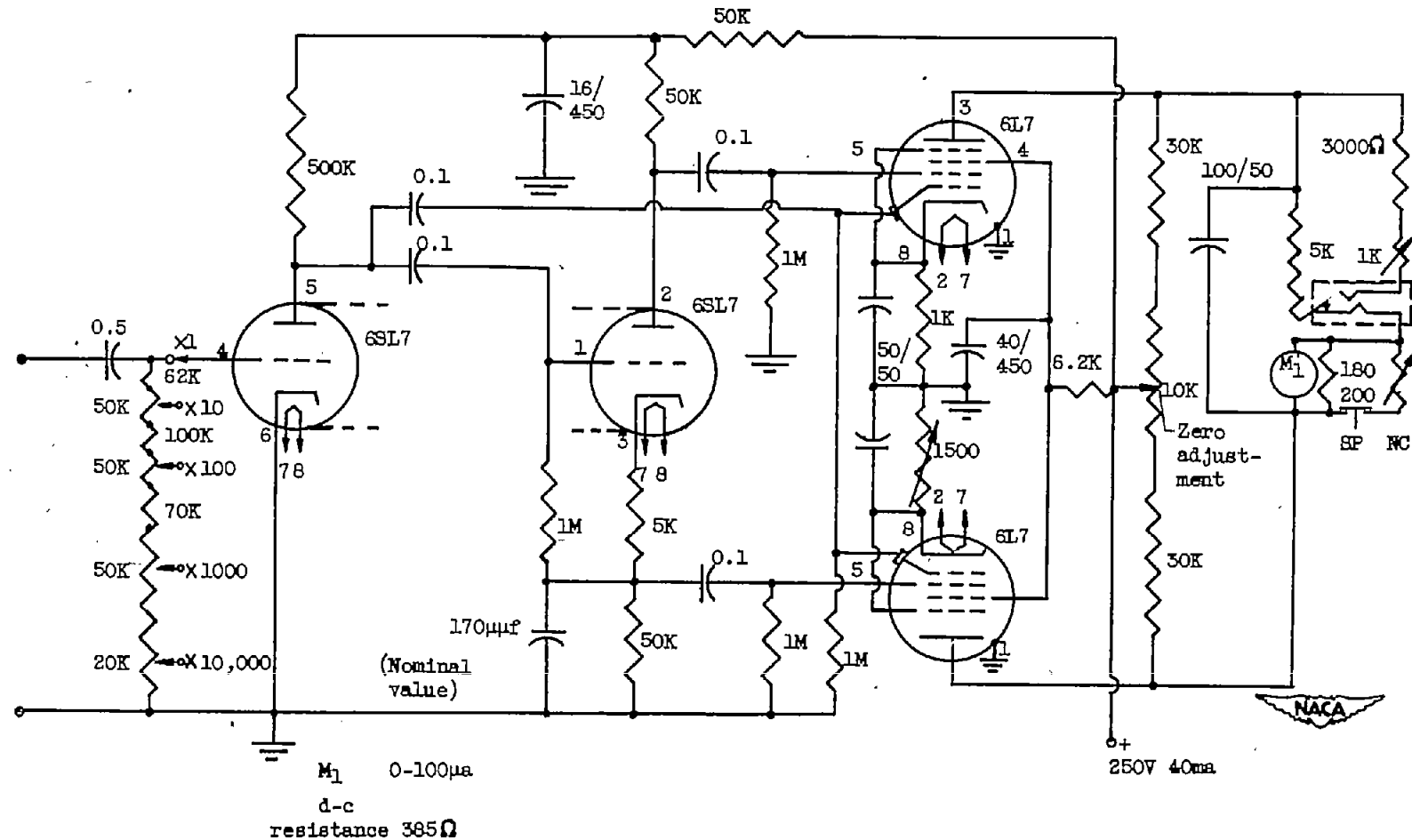


Figure 9. - Simplified diagram of average-square computer.



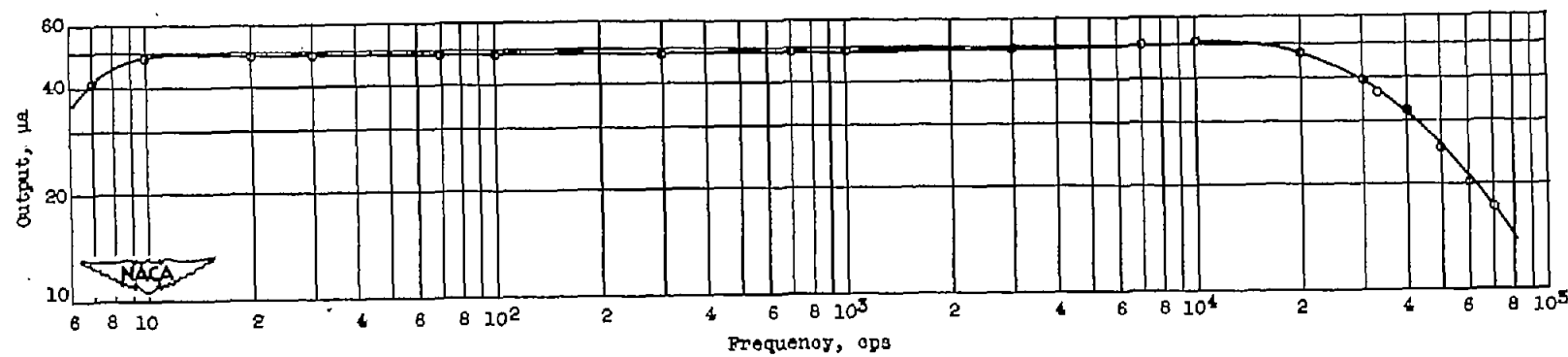


Figure 11. - Average-square computer; number 2 frequency response. Input voltage, 5.

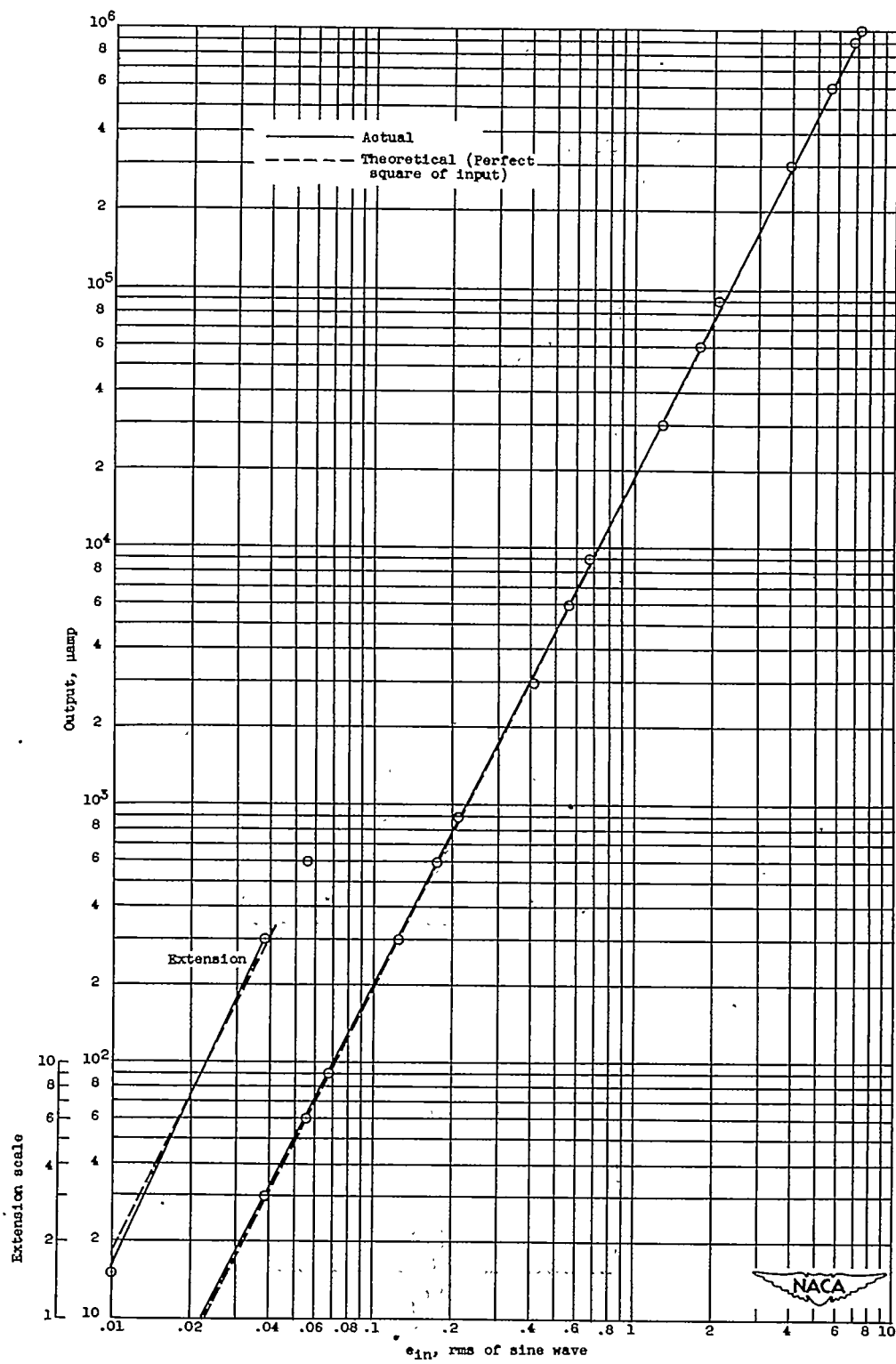


Figure 12. - Calibration for average-square computer number 2.

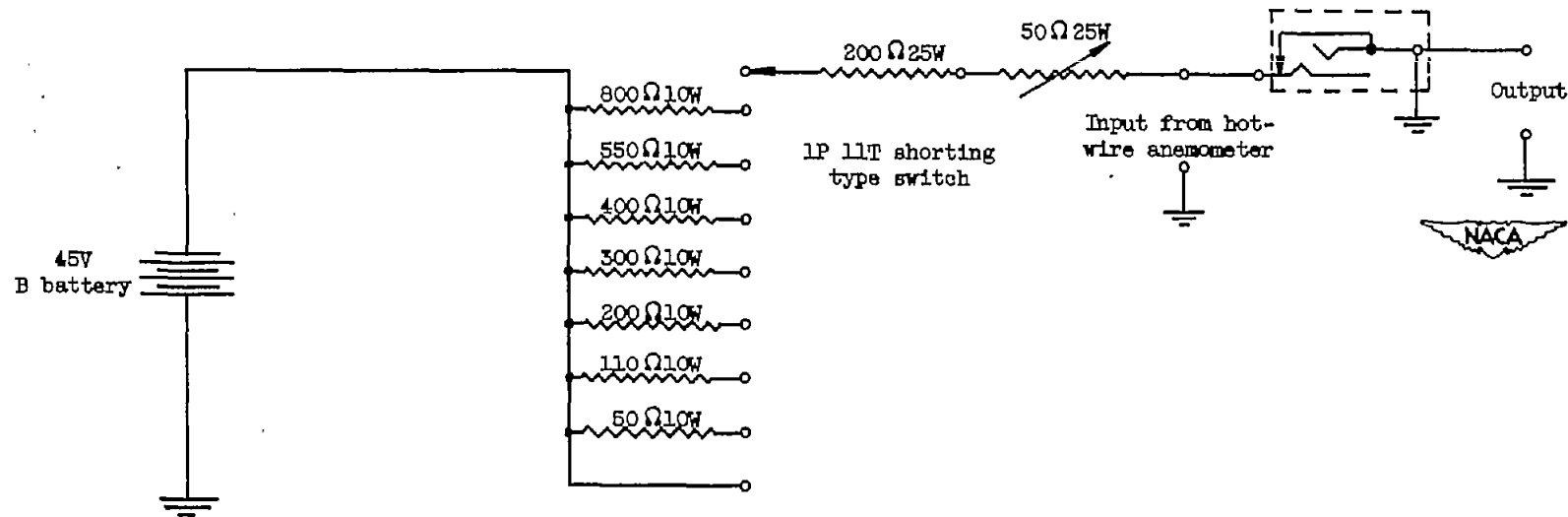


Figure 13. - Auxiliary current supply for hot-wire anemometer.

NACA TN 2843

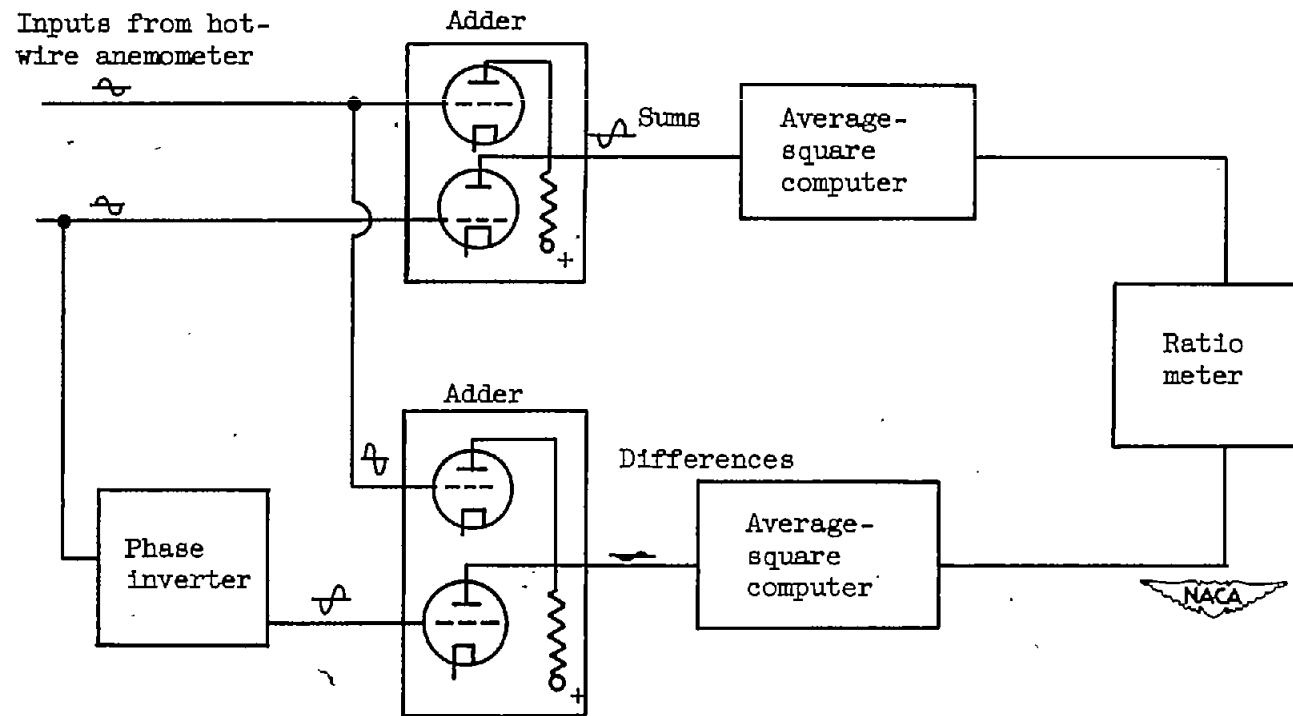


Figure 14. - Simplified diagram of double-correlation computer.

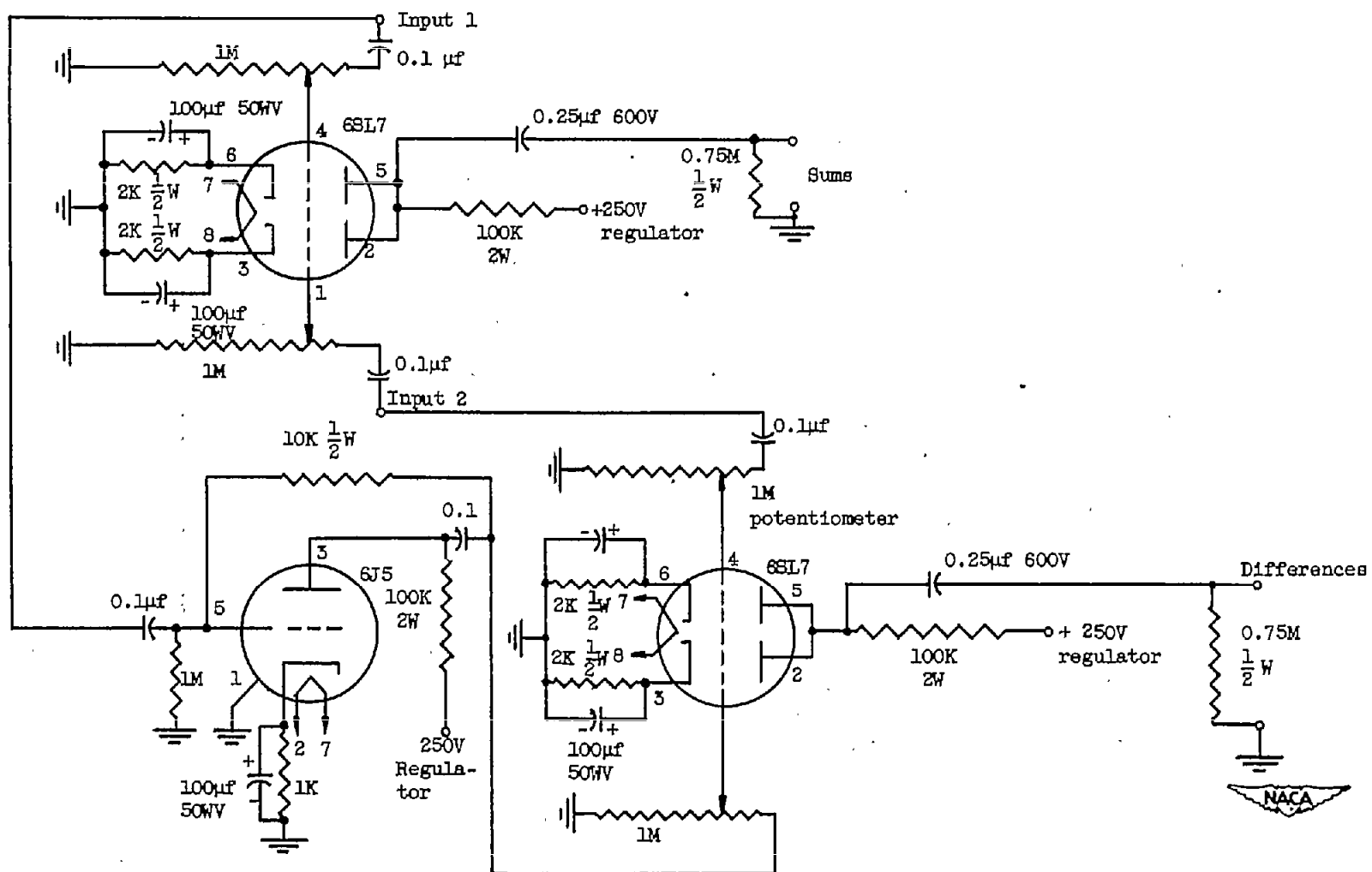


Figure 15. - Sums and differences circuit for double-correlation computer.

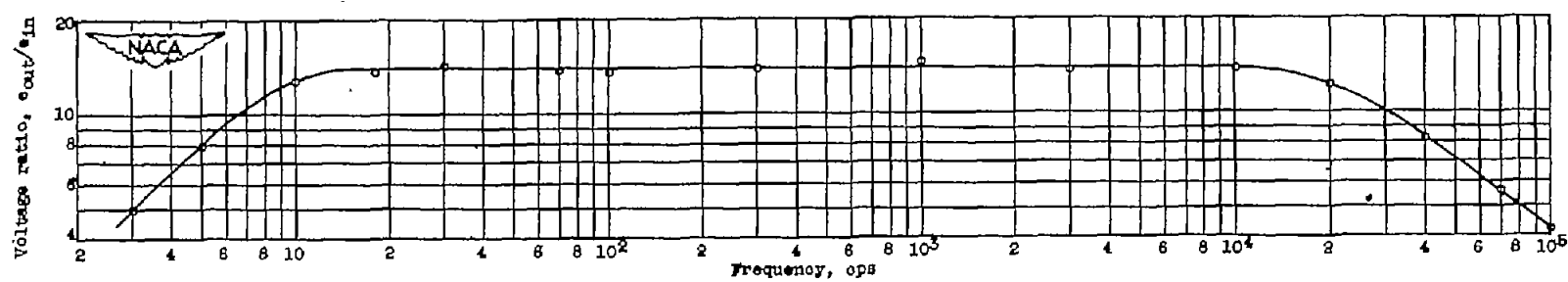


Figure 16. - Frequency response for double-correlation computer.

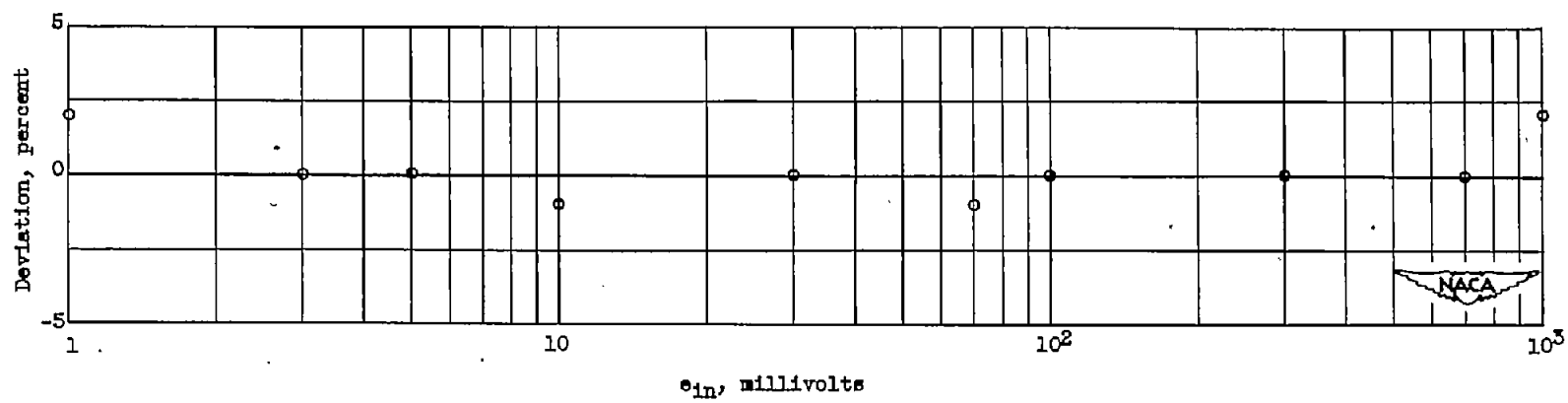


Figure 17. - Deviation of gain with amplitude for double-correlation computer.

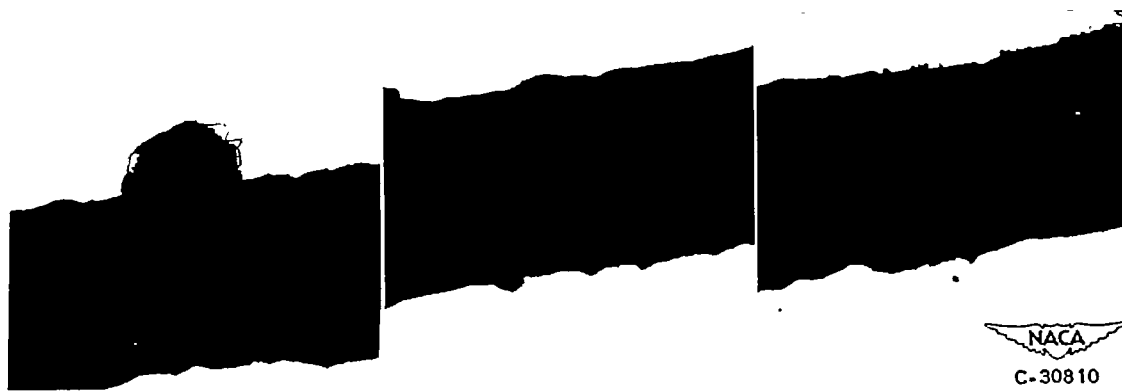
2640



(a) Sample A; etched tungsten; nominal diameter, 0.0002 inch; actual diameter, 0.000248 inch; X5064.



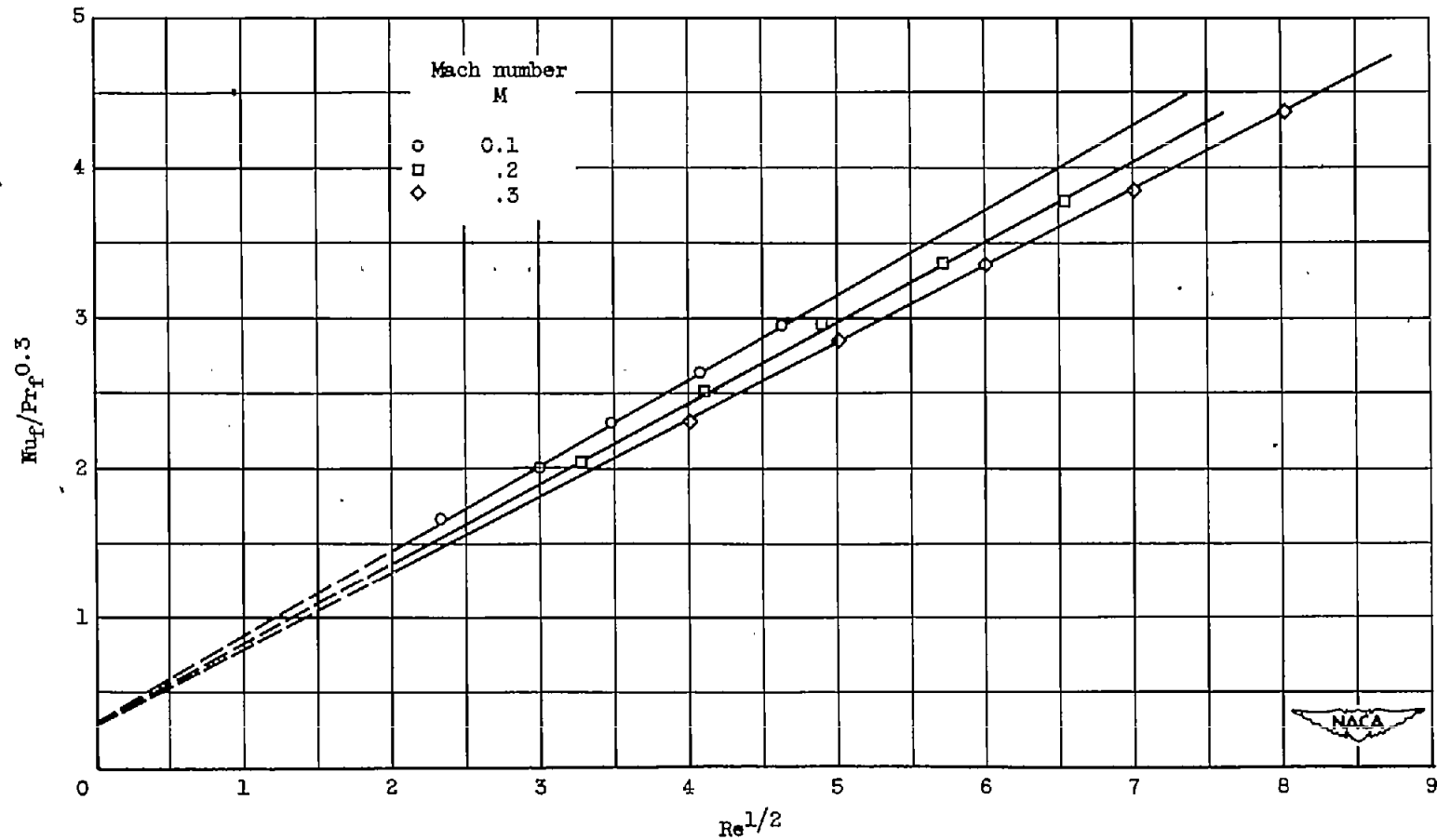
(b) Sample B; etched tungsten; nominal diameter, 0.0002 inch; actual diameter, 0.000199 inch; X5450.



NACA
C-30810

(c) Sample C; etched tungsten; nominal diameter, 0.00014 inch; actual diameter, 0.000181 inch; X5420.

Figure 18. - Electron micrographs of etched tungsten wire supplied by two manufacturers.



(a) Wire temperature, 215° F.

Figure 19. - Heat-loss correlation for 0.0002-inch-diameter tungsten wire. Length-diameter ratio, 2500; total temperature, 75° F.

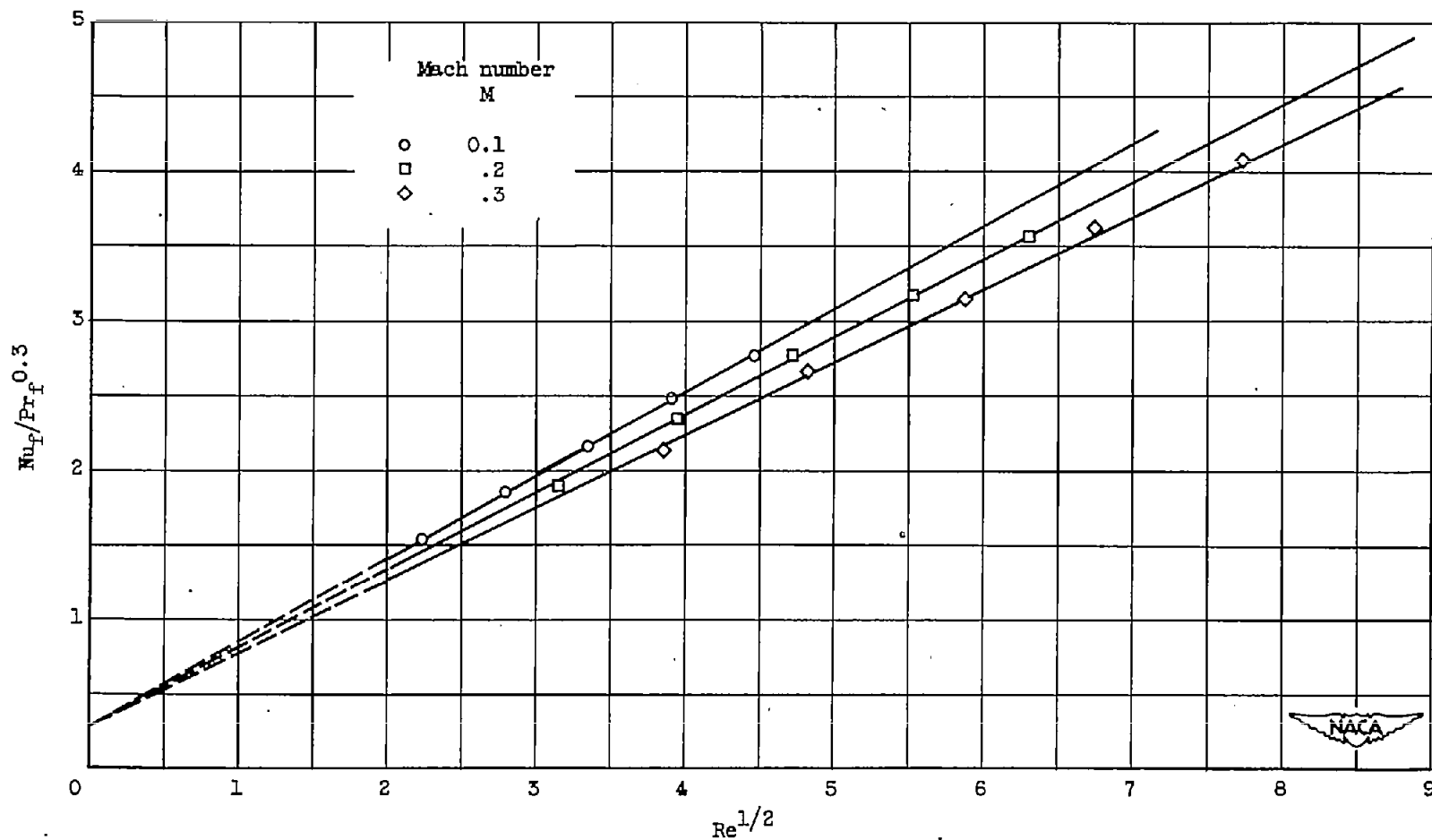
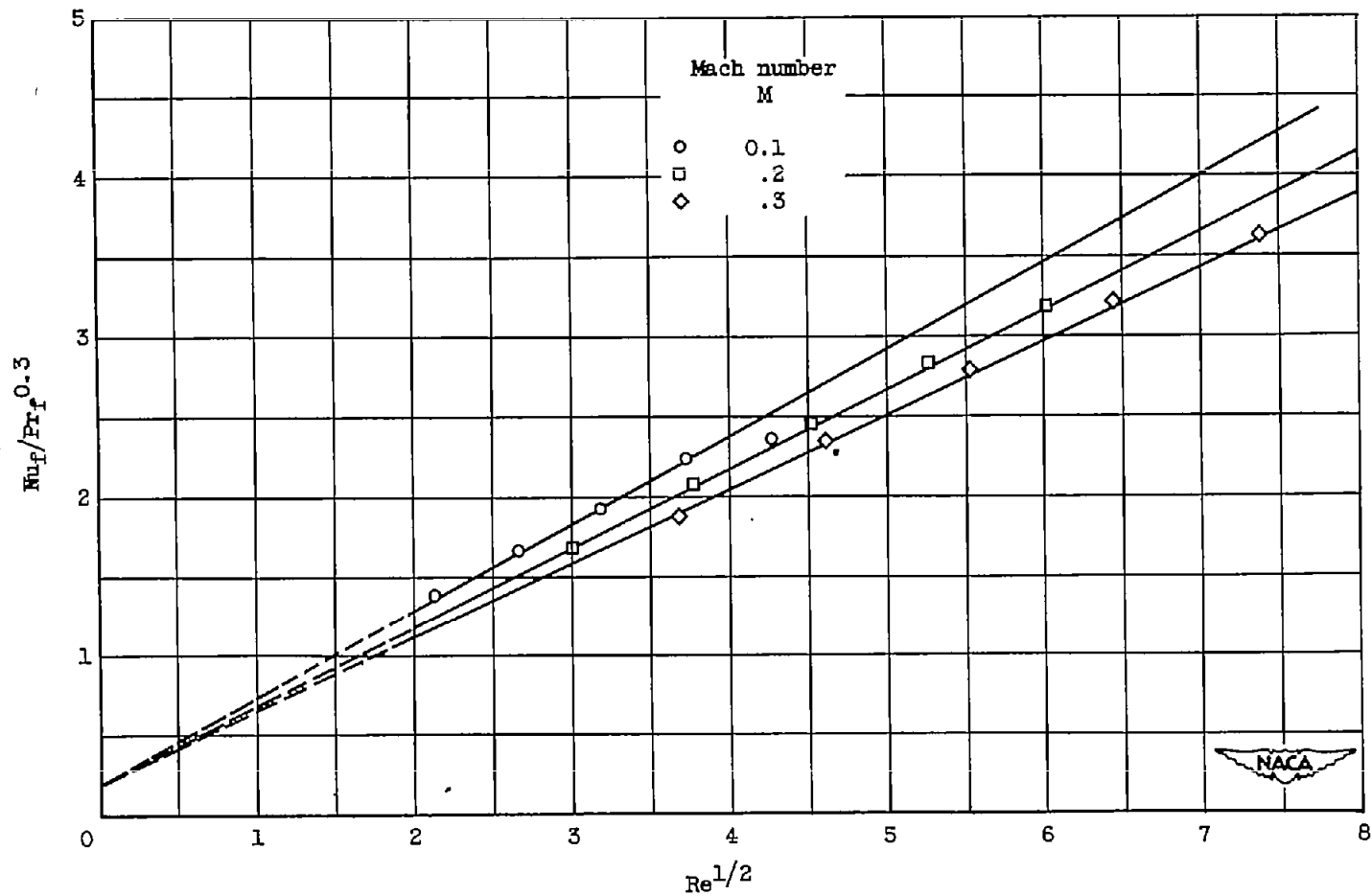
(b) Wire temperature, 345° F.

Figure 19. - Continued. Heat-loss correlation for 0.0002-inch-diameter tungsten wire. Length-diameter ratio, 2500; total temperature, 75° F.



(c) Wire temperature, 528° F.

Figure 19. - Concluded. Heat-loss correlation for 0.0002-inch-diameter tungsten wire. Length-diameter ratio, 2500; total temperature, 75° F.

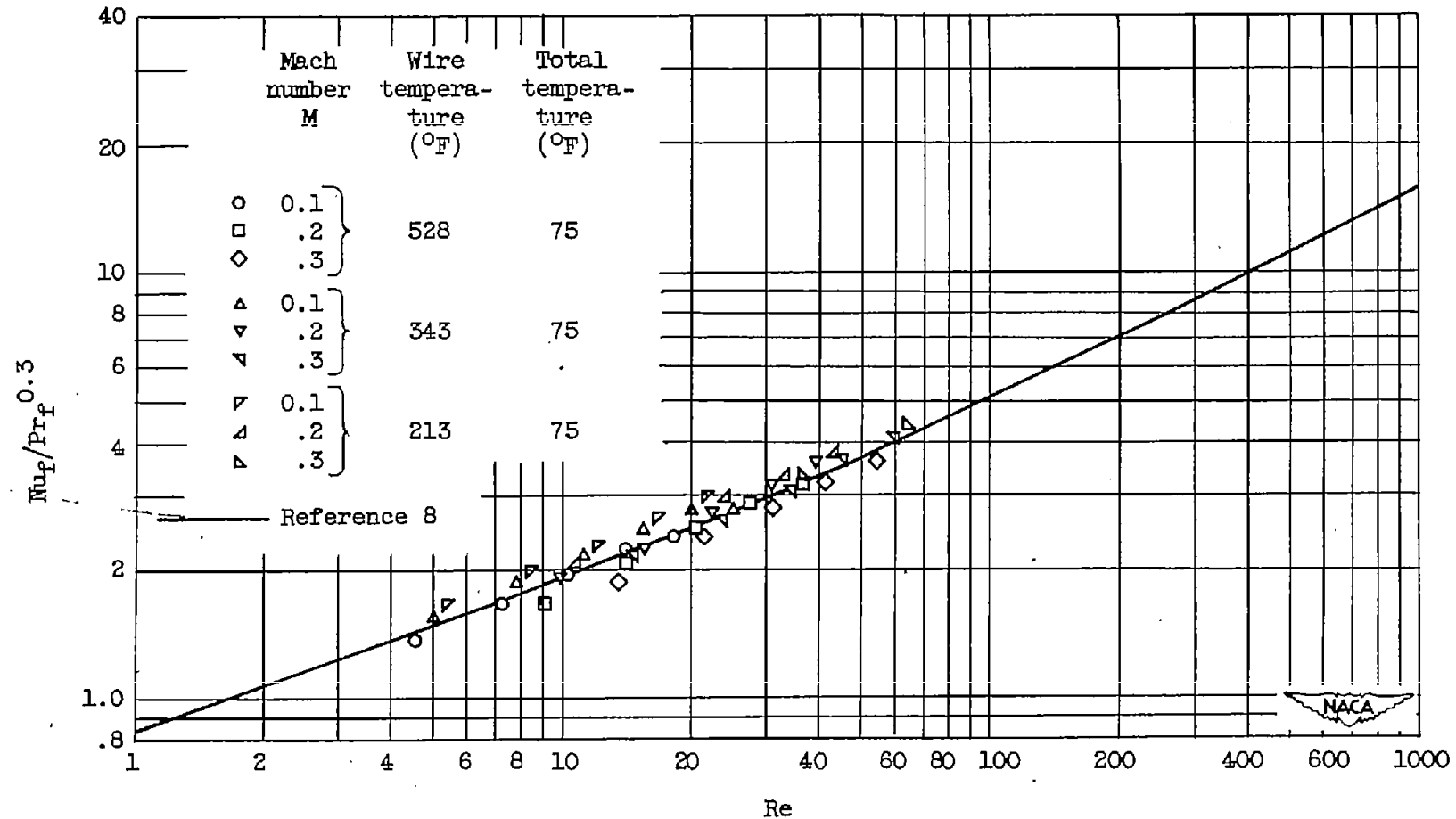


Figure 20. - Heat-loss correlation; comparison of data with data of reference 8. Tungsten wire; diameter, 0.0002 inch; length-diameter ratio, 2500.

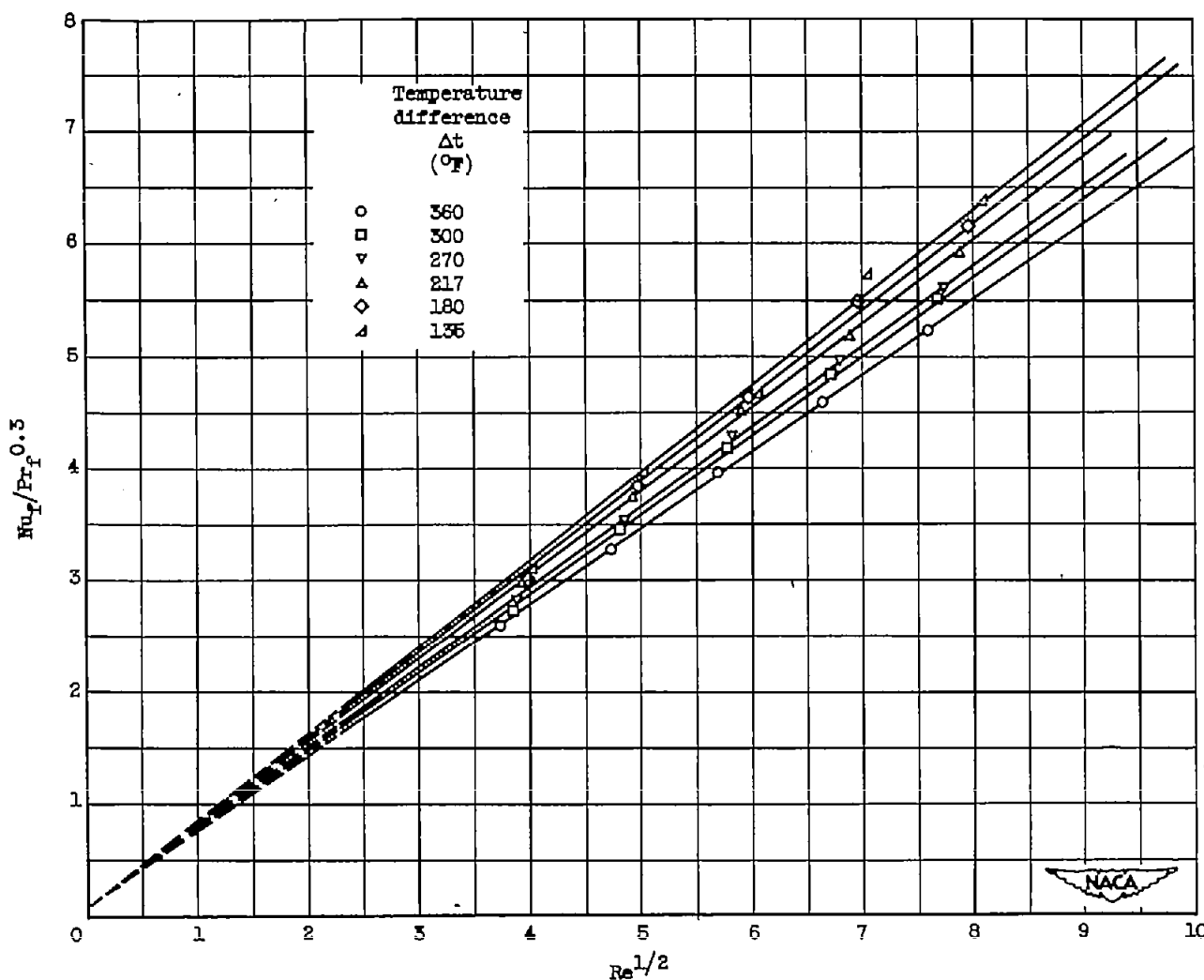


Figure 21. - Effect of temperature difference between wire and air stream on heat loss. Tungsten wire; diameter, 0.0002 inch; length, 0.080 inch; Mach number, 0.3.

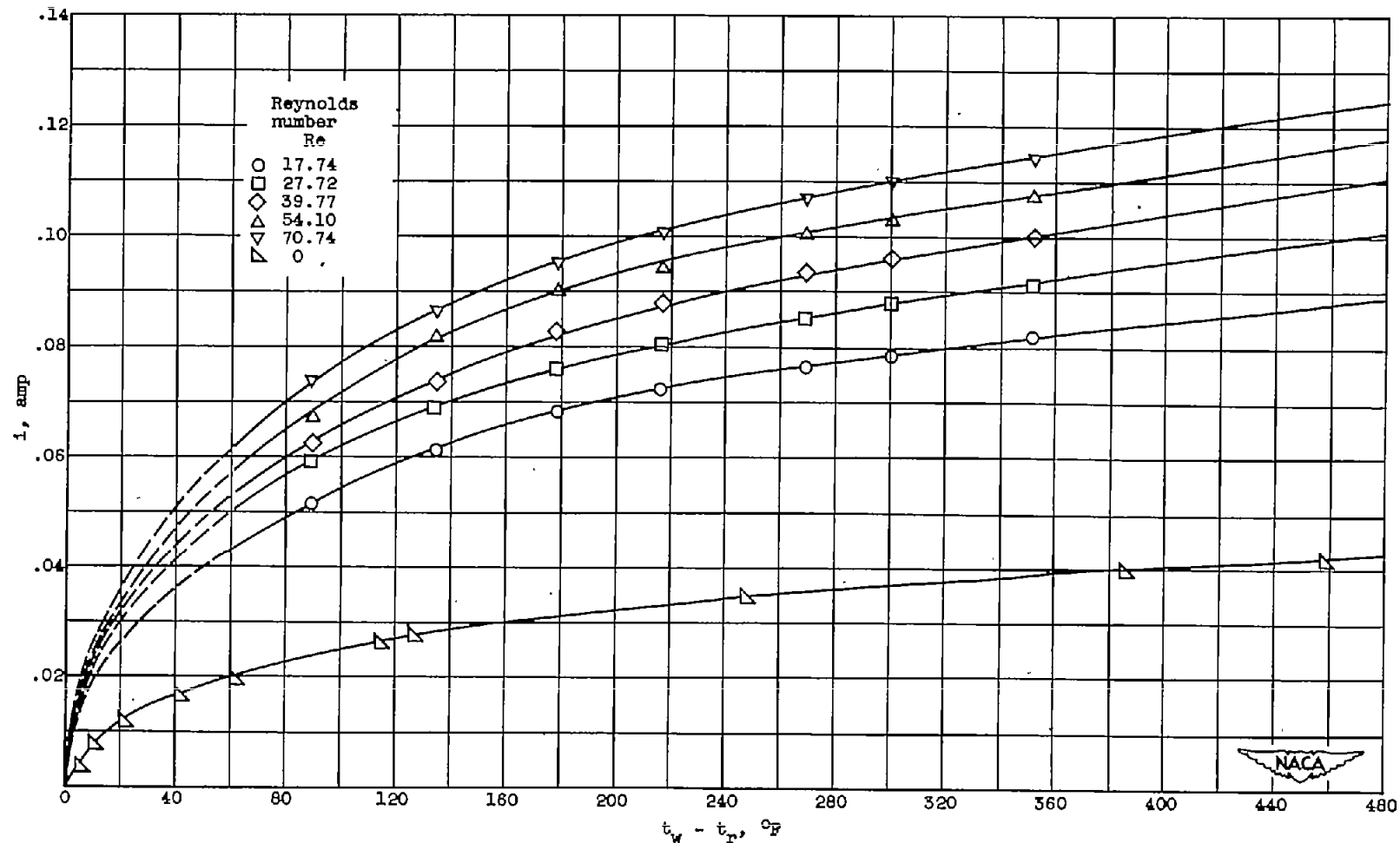


Figure 22. - Variation of current with temperature of hot wire for constant Reynolds number. Tungsten wire; diameter, 0.0002 inch; length, 0.078 inch; Mach number, 0.3.

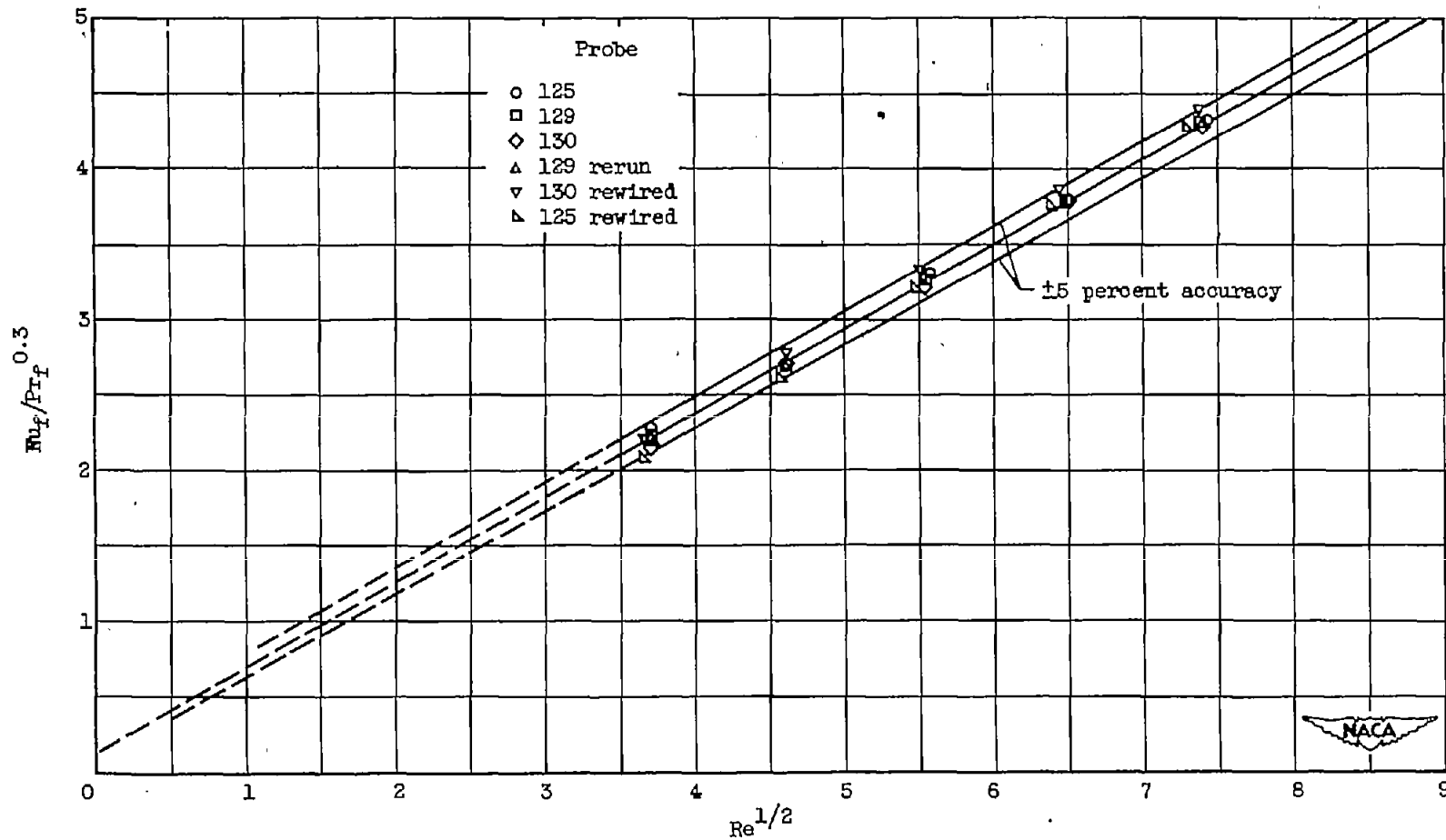


Figure 23. - Comparison of calibrations of 0.0002-inch-diameter tungsten wires of 0.080-inch length. Mach number, 0.3; total temperature, 80° F; wire temperature, 490° F.

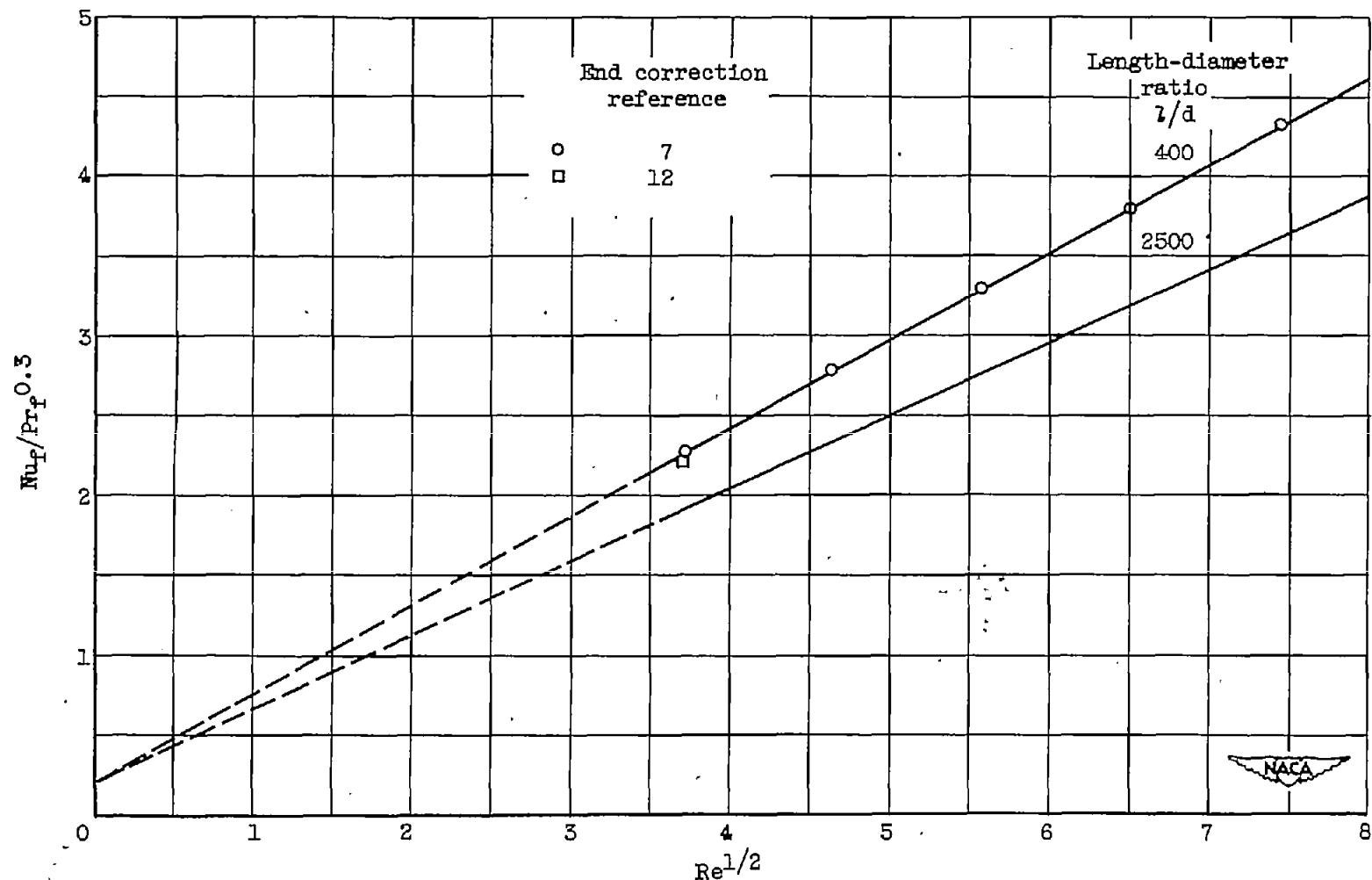
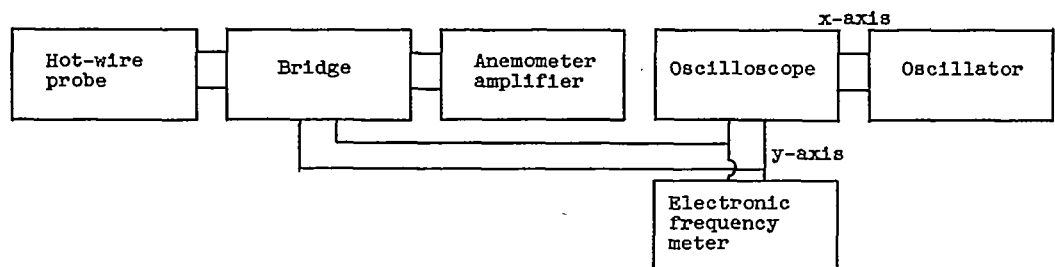
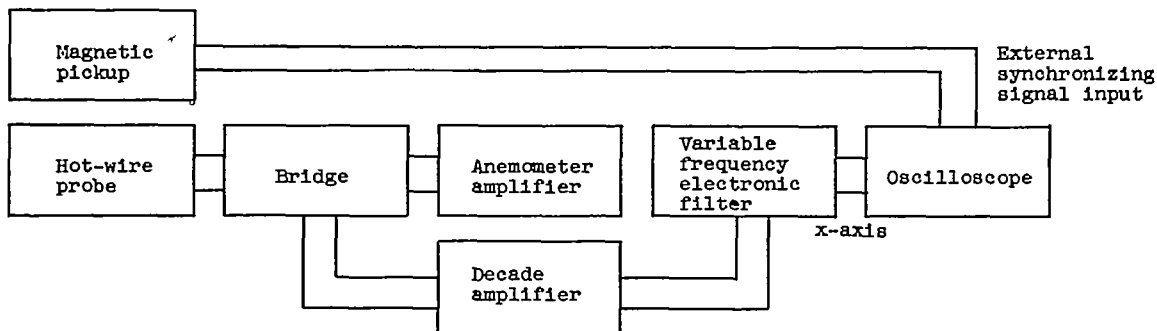


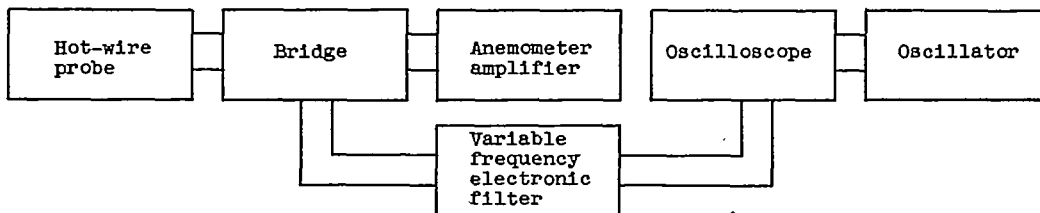
Figure 24. - Comparison of heat loss from two 0.0002-inch-diameter tungsten wires of different length-diameter ratios. Mach number, 0.3.



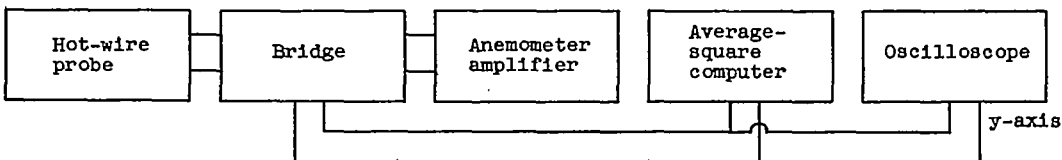
(a) Frequency measurements.



(b) Velocity profile measurements.

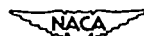


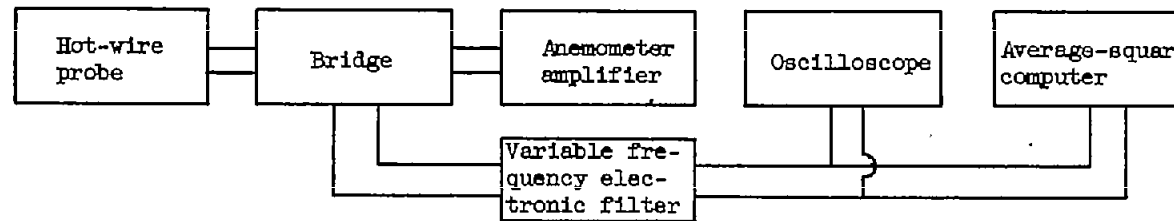
(c) Compressor surge and rotary stall measurements.



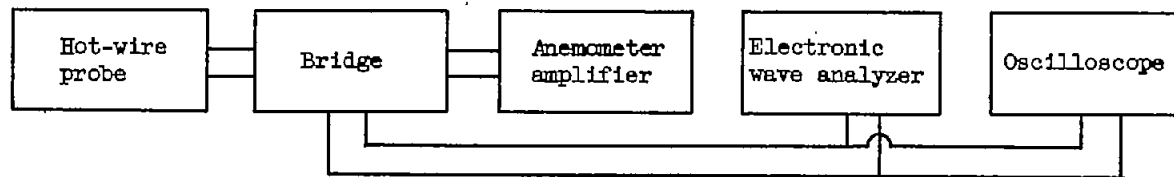
(d) Intensity measurements.

Figure 25. - Block diagram of instrumentation hookups.

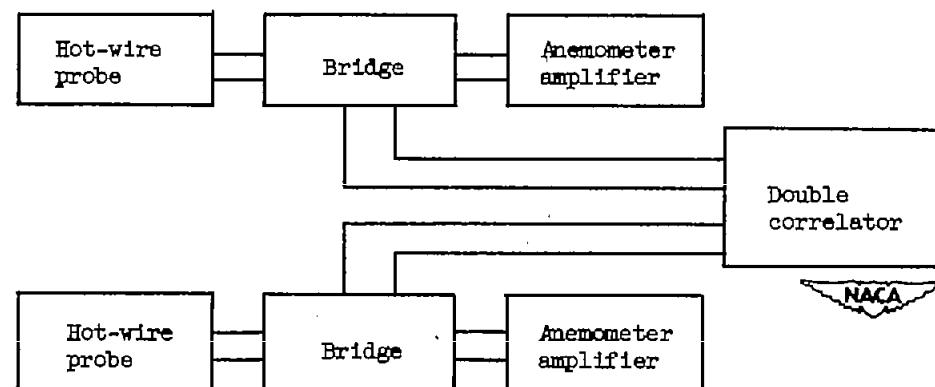




(e) Spectrum of turbulence measurements (method 1).

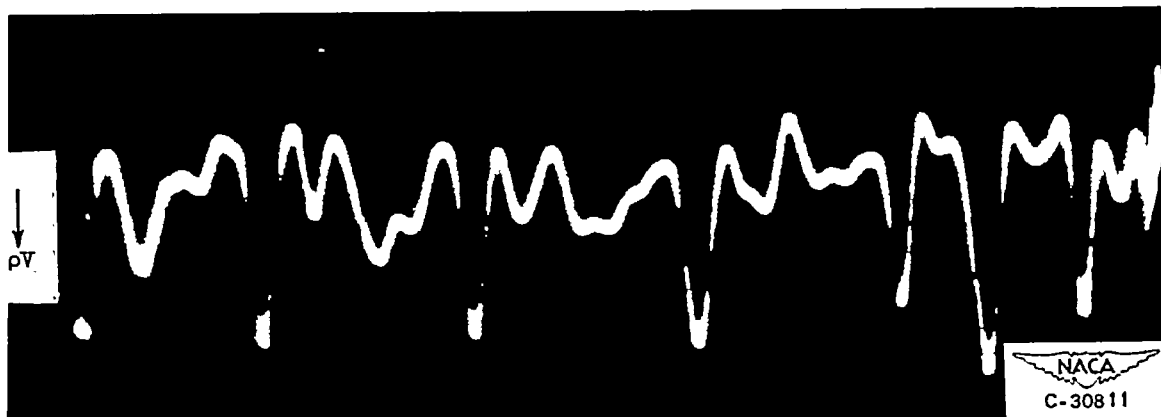


(f) Spectrum of turbulence measurements (method 2).



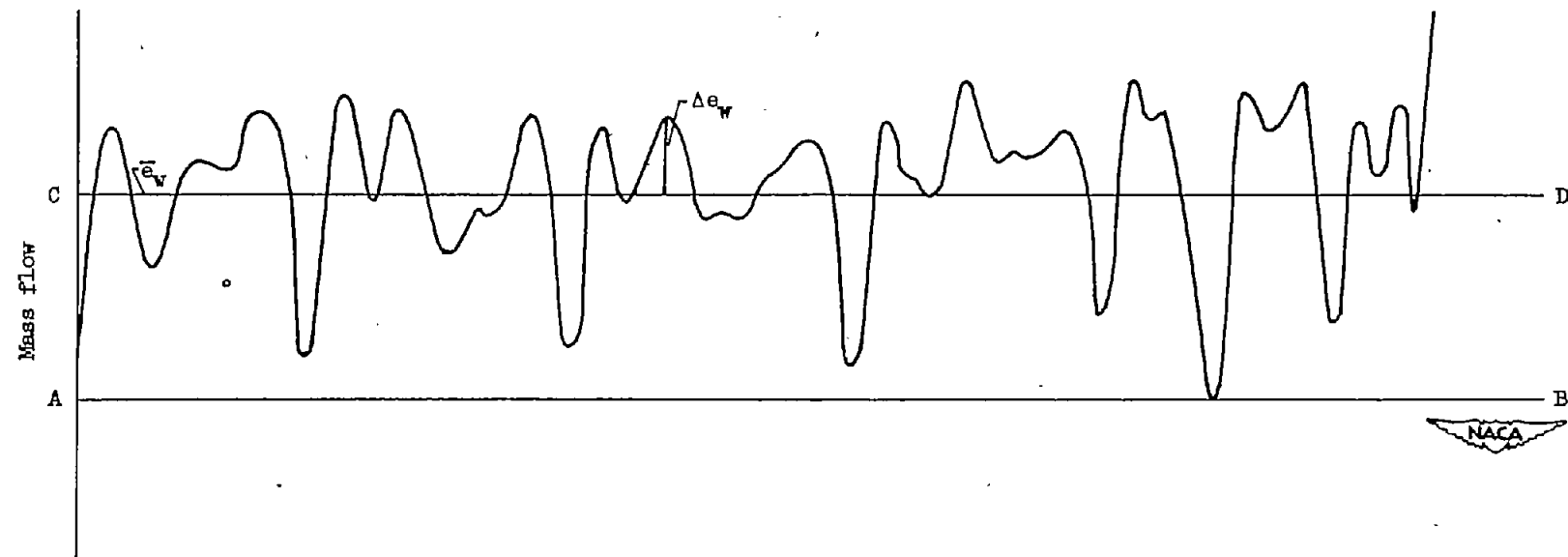
(g) Scale of turbulence measurements.

Figure 25. - Concluded. Block diagram of instrumentation hookups.



(a) Oscillogram.

Figure 26. - Velocity profiles from 48-inch centrifugal compressor.



(b) Trace of oscillogram, showing method of locating mean flow line.

Figure 26. - Concluded. Velocity profiles from 48-inch centrifugal compressor.

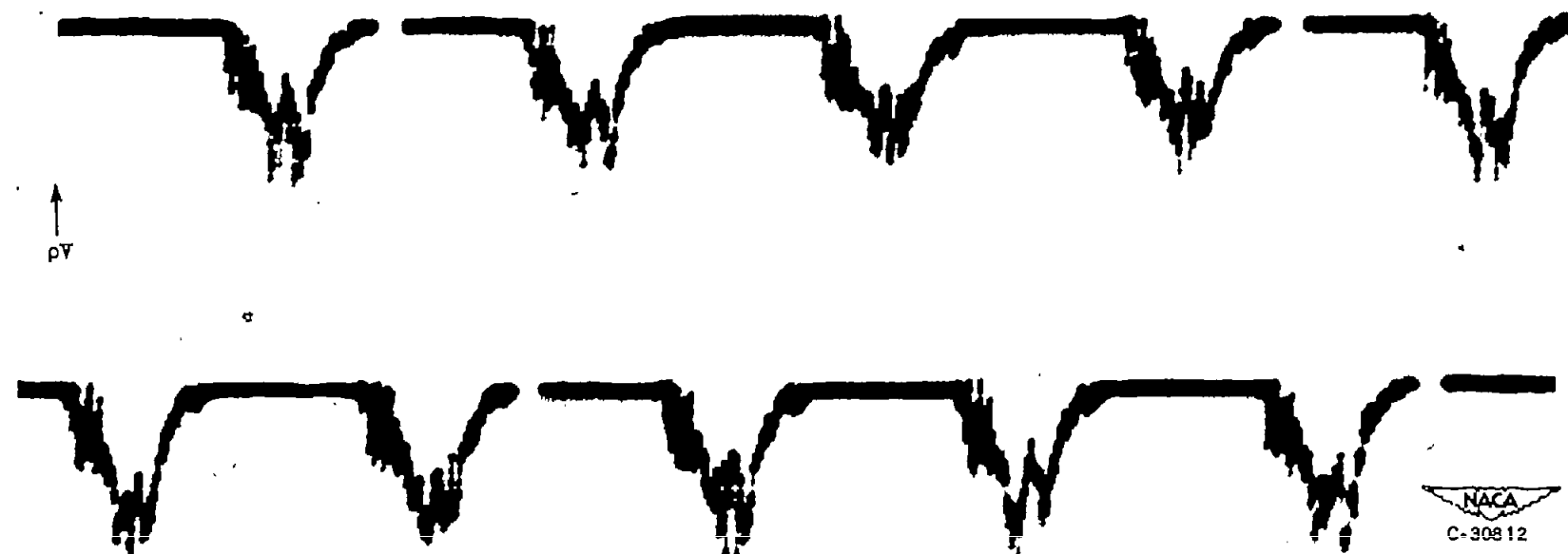


Figure 27. - Hot-wire signals from a single-stage axial-flow compressor with five rotating stall regions.

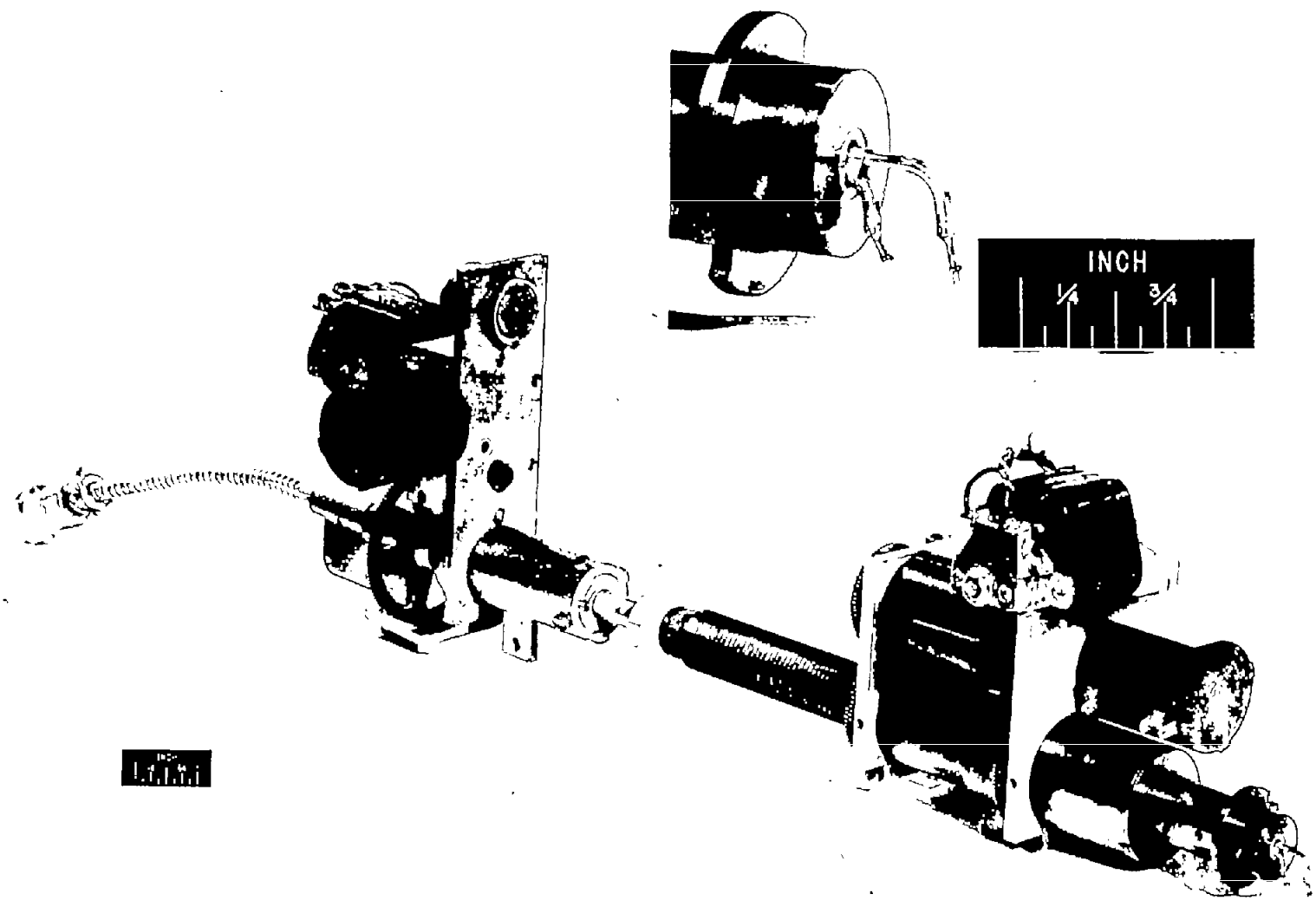


Figure 28. - Double-correlation probe and actuators.

C-29882

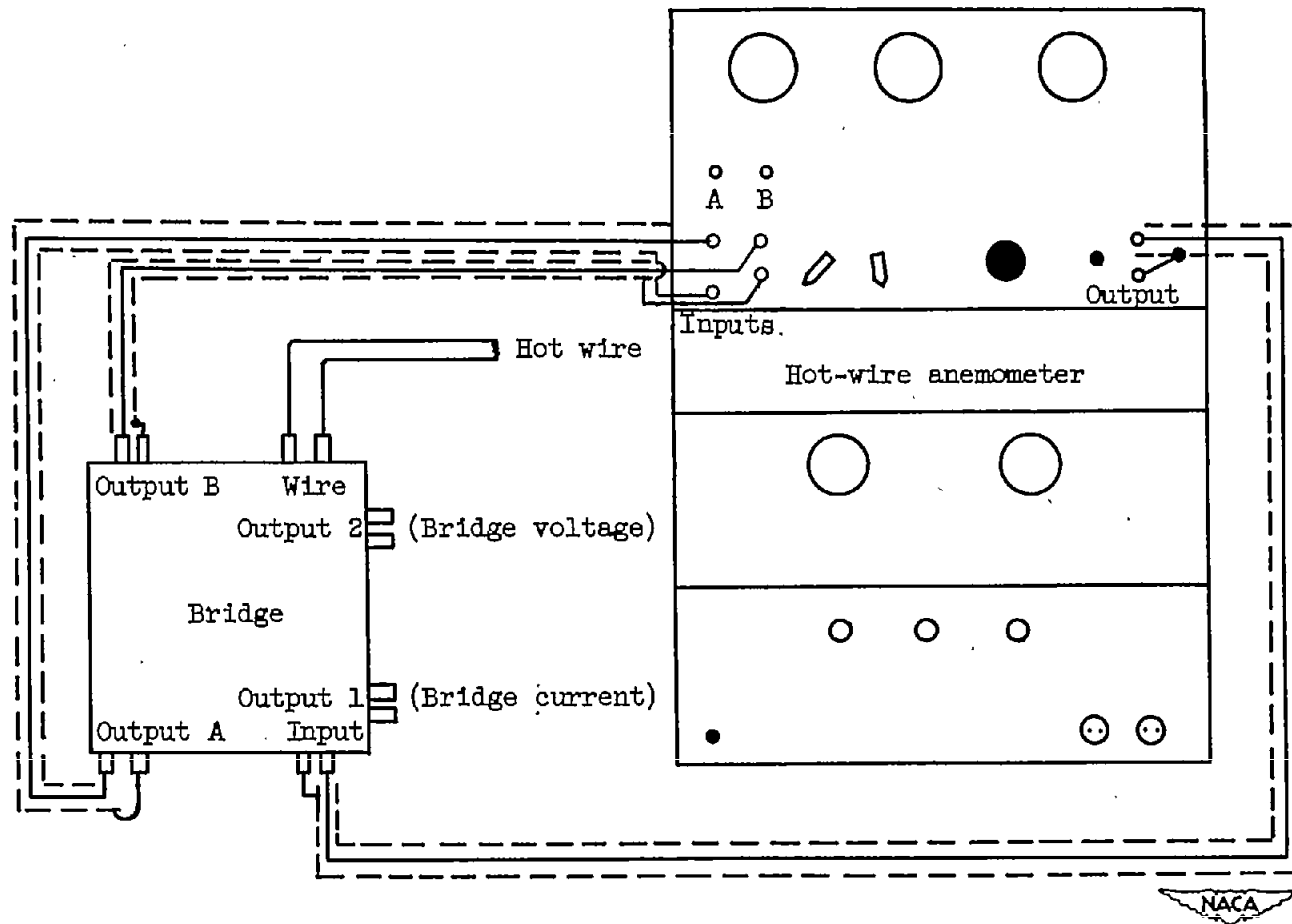


Figure 29. - Hot-wire anemometer to bridge connections.

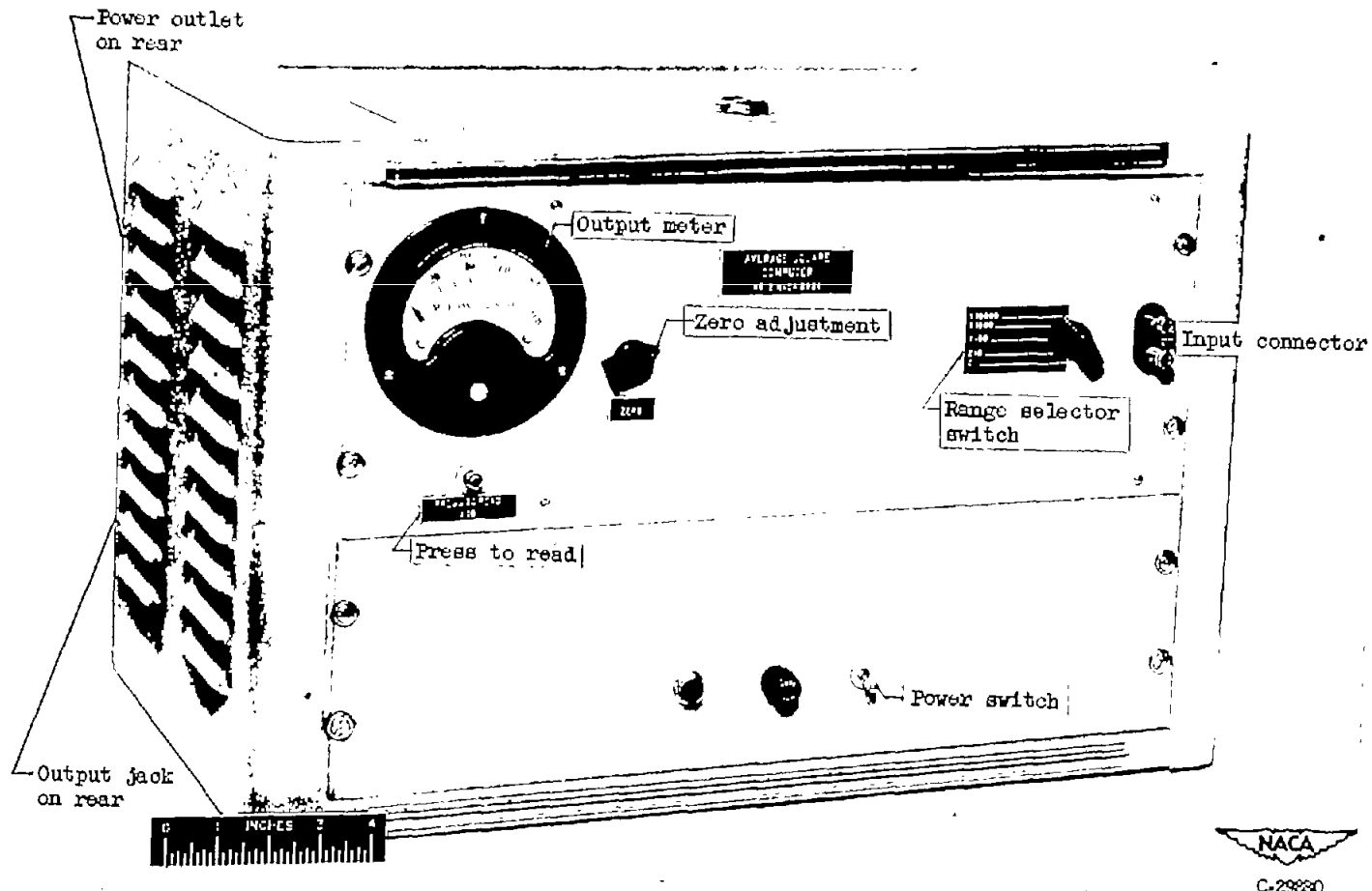


Figure 30. - Average-square computor.

NACA
C-2880

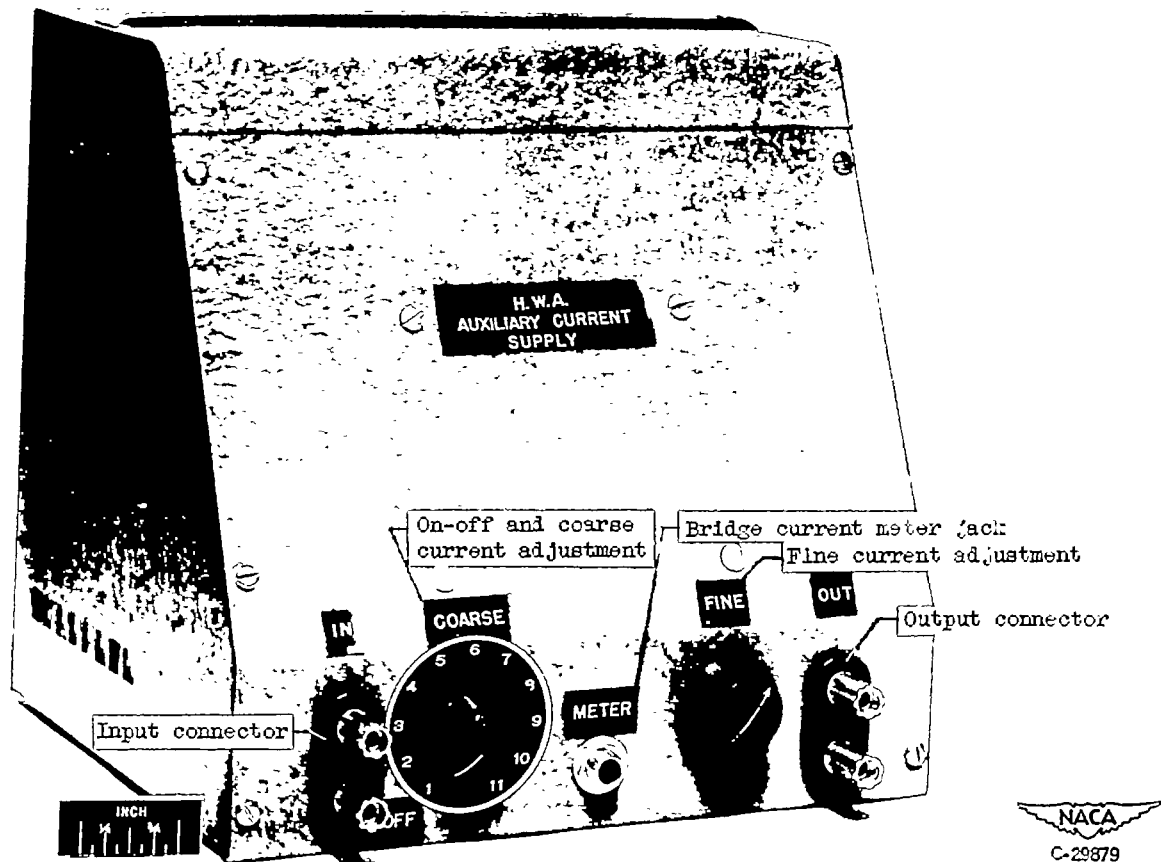


Figure 31. - Auxiliary current supply.

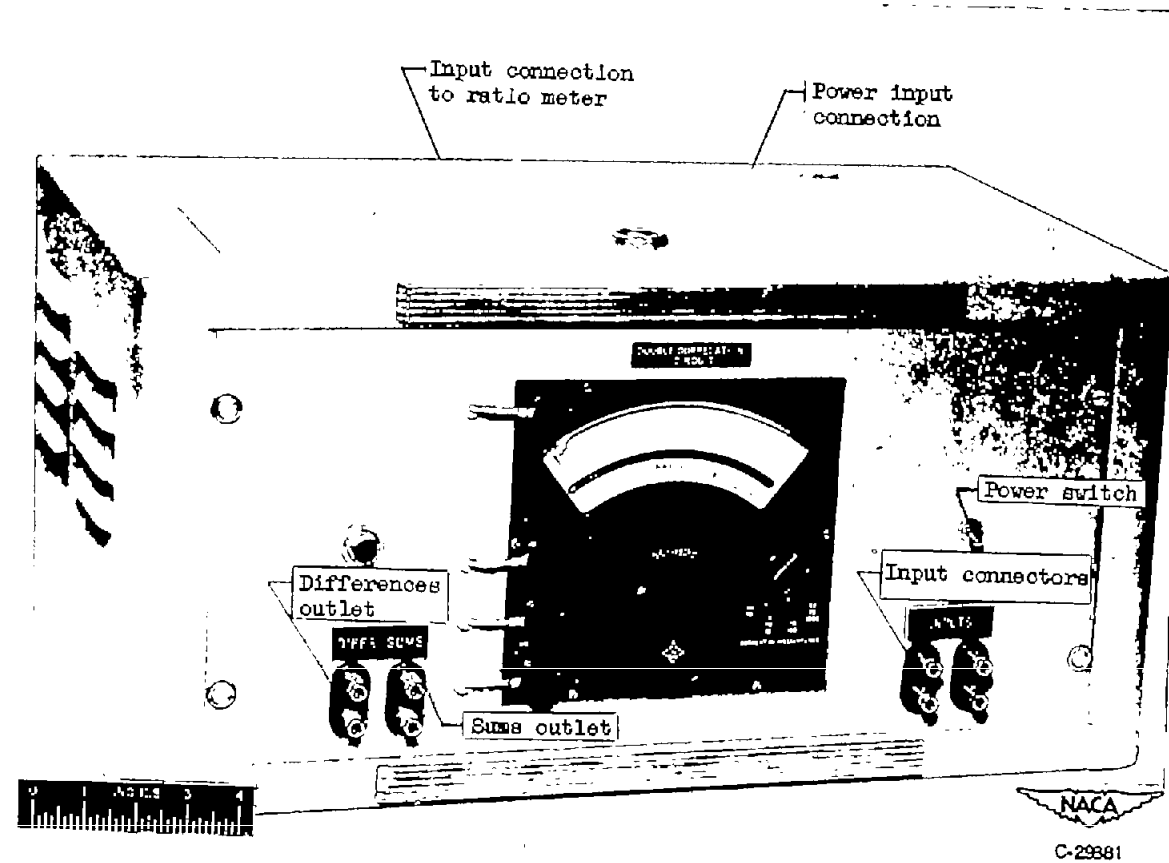


Figure 32. - Double-correlation instrument.

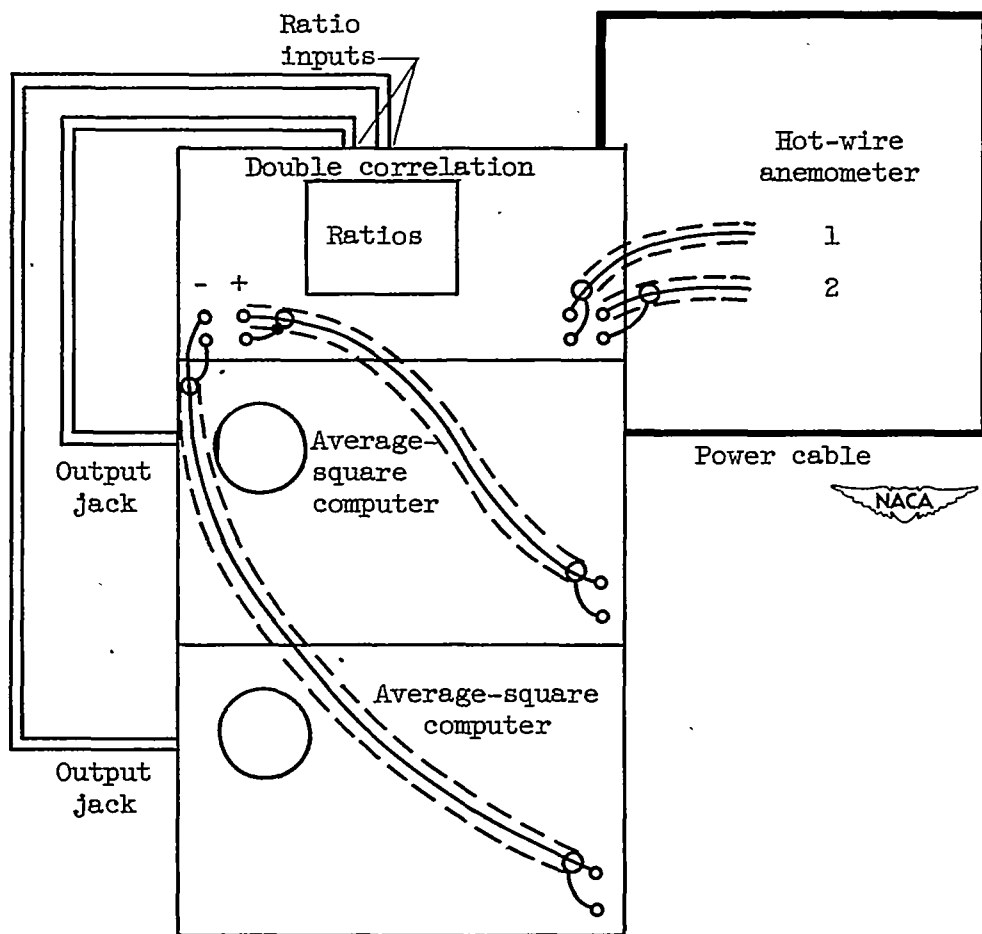


Figure 33. - Double-correlation instrument hookup.

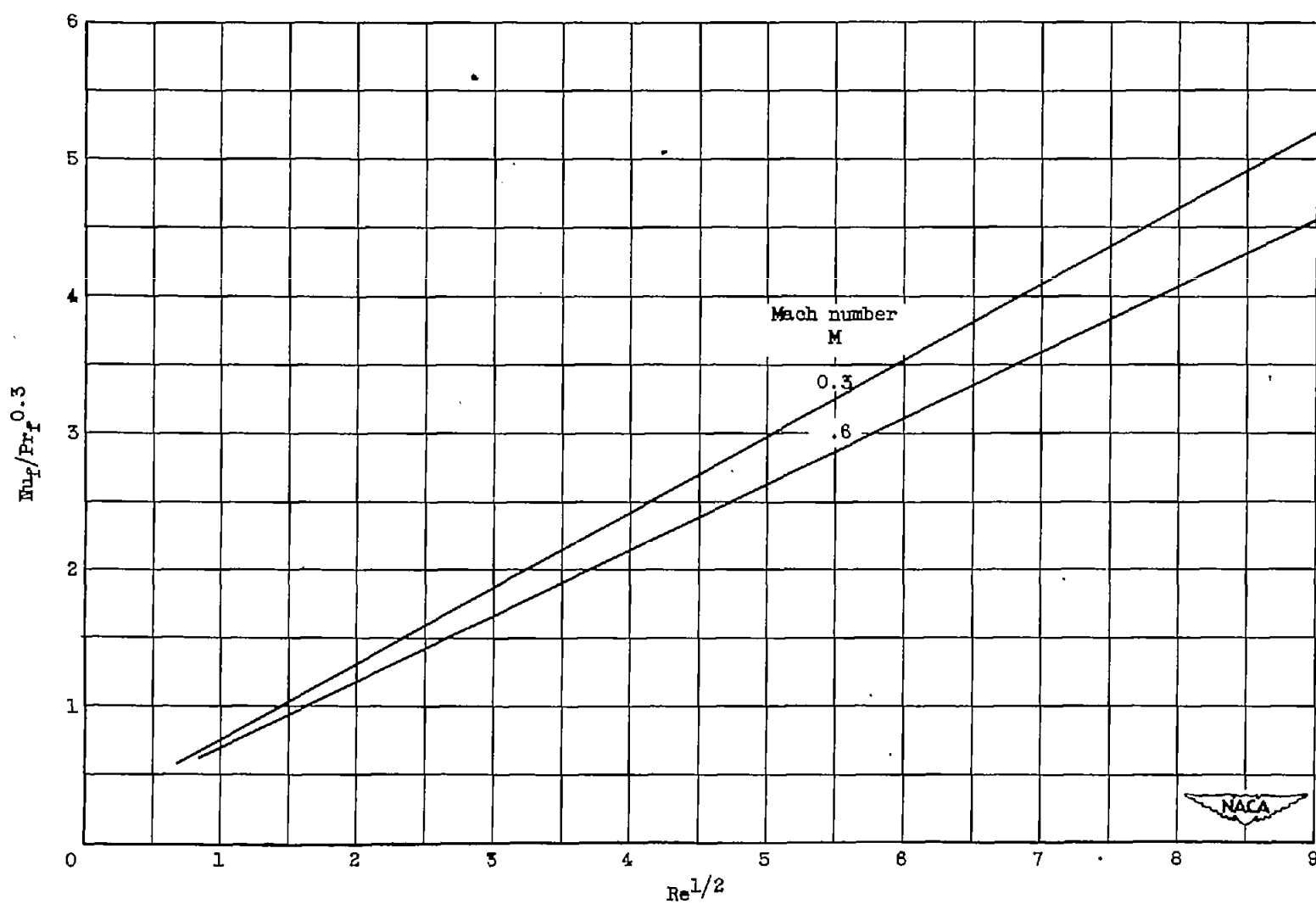


Figure 34. - Calibration curves for hot-wire anemometer probes.